Graphical Abstract

RAFT Unchained — Scalable Manufacturing Of Thiocarbonyl Chain Transfer Agents

Vivek Garg, Anna McCaslin, Michael J. Forrester, Baker W. Kuehl, Sharan Raman, Dhananjay Dileep, Eric W. Cochran

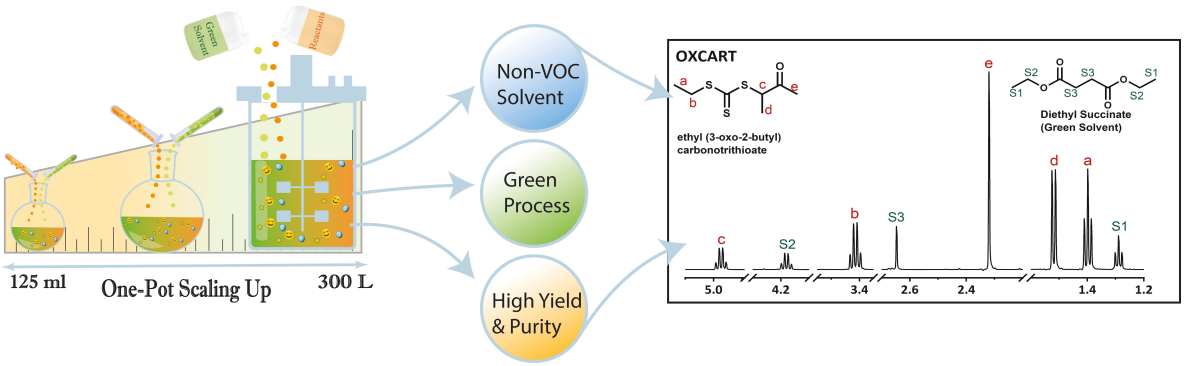

Highlights

RAFT Unchained — Scalable Manufacturing Of Thiocarbonyl Chain Transfer Agents

Vivek Garg, Anna McCaslin, Michael J. Forrester, Baker W. Kuehl, Sharan Raman, Dhananjay Dileep, Eric W. Cochran

- Facile one-pot scalable approach to synthesize chain transferring agents for RAFT polymerization.
- Use of Non-Volatile organic solvents/green solvents to synthesize these molecules.
- High purity and yield of the molecules, with no separation involved.
- RAFT equilibrium is maintained throughout the polymerization and the process provides avenues to make functional polymers accessible universally.

RAFT Unchained — Scalable Manufacturing Of Thiocarbonyl Chain Transfer Agents

Vivek Garg, Anna McCaslin, Michael J. Forrester, Baker W. Kuehl, Sharan Raman, Dhananjay Dileep, Eric W. Cochran[a,*]

[a]*Department of Chemical & Biological Engineering, Iowa State University, 50011, Ames, UA, United States*

Abstract

Here, we report an efficient approach for the manufacturing of chain-transfer agents (CTA) for RAFT polymerization using non-volatile organic compounds (VOC) in one pot with only water-washing as a work-up. Although the RAFT process is scientifically mature, nearly all RAFT CTAs are still produced through multi-step syntheses involving material- and energy-intensive separations. Today's commercially available RAFT agents are high-value specialty products available only from fine chemical vendors, limiting RAFT's industrial success. The current work illustrates a single-step one-pot approach to synthesize ethyl (3-oxo-2-butyl) carbonotrithioate and O-ethyl S-(3-oxobutan-2-yl) carbonodithioate at up to 10 L scale in various non-VOC solvents with varied degrees of potential for cross-reactivity: diethyl succinate, tributyl acetyl citrate, castor oil glycidal ether, and glycerol triglycidyl ether. We studied the purity and yield of these CTAs using NMR and LC-MS, and then conducted rigorous polymerization and kinetic studies to evaluate the efficacy of these molecules in maintaining the RAFT equilibrium. We found that the use of these non-VOC solvents impedes neither the synthesis of these molecules nor the RAFT control, thus enabling scalable and low-impact pathways to RAFT CTA manufacturing.

Keywords: One-pot, Green Solvent, Scalable Process, Chain Transferring Agents, Reversible Addition-Fragmentation Chain Transfer

1. Introduction

Over recent decades, significant advancements have been made in the research and synthesis of well-defined functional polymers [1, 2, 3]. The appeal of these materials lies in their customizable chemical, physical, and biological properties, which make them highly versatile for various applications [4, 5]. However, transitioning these materials to commercial production remains a challenge, primarily due to the high cost

*Corresponding author

of reagents, stringent synthesis protocols, and the energy-intensive separation and purification processes required to produce the final product. Notably, block copolymers (BCPs) exemplify such high-value specialty products that have seen limited commercial success. Currently, the most commercially relevant block copolymers are limited to styrenic-olefinic blocks produced through anionic polymerization, representing a mere 0.05% of the total plastic market share [6]. These BCPs, despite their versatility and high tunability, are confined to only a few polymer types:-styrene-butadiene, styrene-isoprene, and styrene-ethylene, due to the limitations of anionic polymerization for polymerizing non-styrenic or olefinic monomers. The reactive anion in the polymerization process interacts unfavorably with the functional groups on these monomers, posing significant challenges, particularly as the industry moves towards bio-derived monomers for developing functional materials [7, 8, 9]. The abundance of biomass offers a rich source of building blocks for creating materials with finely tuned properties [10]. Exploring these biobased monomers within the realm of block copolymers (BCPs) facilitates the development of entirely new and extraordinary materials. Although a significant body of research highlights the exceptional qualities of biobased-acrylic BCPs, achieving scalability for these materials has remained a big challenge [11, 12].

The production of BCPs primarily relies on anionic polymerization, with ring-opening polymerization accounting for only a small fraction of the industry [7, 6]. These methods are limited in their ability to handle a diverse range of monomers, restricting the commercial availability of functional polymers. In contrast, free radical polymerization (FRP) offers more flexibility for polymerizing various functional monomers but lacks the precision needed to create complex polymeric architectures [13]. Consequently, there has been substantial progress in developing controlled radical polymerization (CRP) techniques, such as reversible addition-fragmentation chain transfer polymerization (RAFT) and macromolecular design via the interchange of xanthates (MADIX), which provide pseudo-living characteristics during radical-induced polymerization [14, 15]. These techniques utilize thiocarbonylthio-based chain transfer agents (CTAs) (Scheme S1) to maintain the active chain centers in a reversible dormant state, allowing precise control over chain length by mitigating radical-radical reactions through a controlled degenerative transfer, which provides the platform to grow segmented chains.

RAFT offers an incredible degree of versatility in terms of monomer choice, solvent selection, and tolerance of impurities, which sets this polymerization technique apart from all the other available CRP methods. An extensive body of literature exists showcasing the technique's prowess in creating diverse and intricate polymeric architectures for targeted applications [16, 17, 18, 19]. In addition to its exceptional

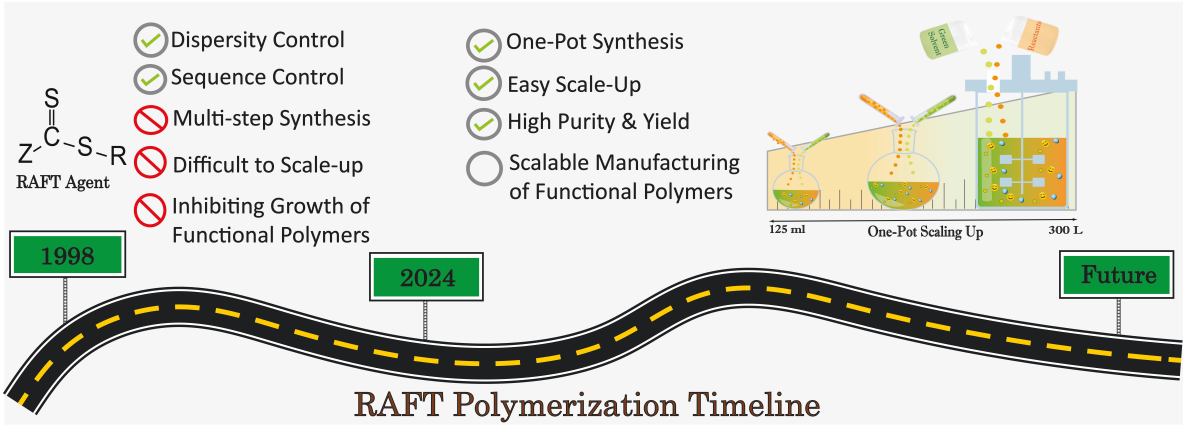

Figure 1: Schematic representing the RAFT timeline and the industrial evolution of functional polymers

control, the CTA offers the potential for incorporating functionality into the polymeric chains, facilitating post-polymerization modifications, grafting, and a wide array of other polymer manipulation techniques, thereby expanding the utility of these polymers in a plethora of applications [20, 21]. Beyond this, RAFT enables the polymerization of monomers that other methods are incapable of handling. RAFT is capable of overcoming both contaminates that would be impractical to remove from biologically sourced monomers, as well as allowing the suppression of gel-point that would typically arise from multifunctional monomers that are almost entirely unavoidable from these feedstocks [22].

Despite all the advantages of RAFT, the widespread industrial adoption of the process has not yet occurred as anticipated [23, 24, 25]. The prolonged time taken by the technique to establish itself in industrial settings has raised concerns regarding its feasibility on a larger scale [26]. The most significant adoption barriers have been the ease in availability of CTAs, difficulty in their synthesis, and their economic feasibility. Even the simplest of these molecules requires time, material, and energy-intensive workup to obtain the pure compound (Figure1 & Figure2a). There is a notable shortage of literature that places significant emphasis on the scalability and production of these molecules. While certain literature does touch upon the subject, the methodologies employed in the work often lack the adaptability required for the process to be called truly "scalable" [27, 28]. This is primarily due to the necessity of separation and purification steps required in obtaining the final product, which confines these molecules to the realm of fine chemicals, with scant commercial offerings in the range of $700-1200/kg at 60–90% purity [26].

In this work, we introduce a green processing technique to synthesize RAFT agents on a large scale. We expand on the synthesis of ethyl (3-oxo-2-butyl) carbonotrithioate (OXCART), a thiocarbonylthio compound developed by Cochran et al. OXCART has demonstrated great potential in terms of widely available precursors and exertion

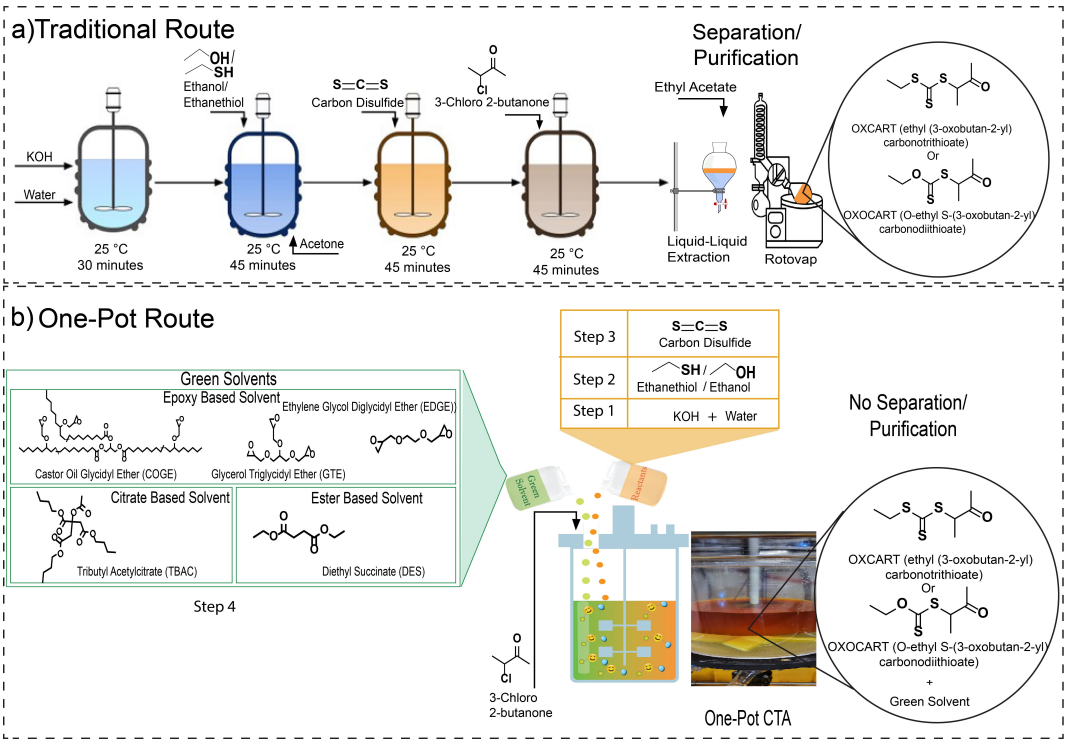

Figure 2: Illustration showing the comparison between a traditional and one-pot scalable synthesis route for CTAs

of excellent RAFT control in polymerizing vinyl aromatics, acrylics, and acrylamides [29]. Its structure was purposefully designed considering the monomer-specific nature of RAFT, which allows it to provide control over a wide class of commercially used monomers. Despite its advantages, the synthesis process faces a notable scalability challenge. The original multi-step synthesis (Figure 2a) necessitated the use of acetone and diethyl ether as organic media, both of which are volatile organic compounds (VOC). These non-reactive media are crucial in promoting nucleophilic substitutions at various stages of the reaction, ensuring favorable reaction kinetics, achieving high product yields, and reaching exacting purity levels. However, the elimination of these VOCs from the final product is essential, as their toxicity necessitates energy-intensive separation processes that significantly increase both overall energy consumption and the production costs of CTA.

To our knowledge, no existing method completely avoids the use of hazardous solvents or circumvents extensive post-synthesis workups. In our study, we address this gap to enhance RAFT's prospects as an industrially practical process. We introduce a non-VOC, scalable, one-pot method for synthesizing OXCART and its xanthate analog OXOCART (O-ethyl S-(3-oxobutan-2-yl) carbonodithioate), effectively eliminating the use of hazardous solvents and obviating the need for post-synthesis cleanup. The large-scale synthesis of a xanthate-based CTA in this work extends RAFT control to vinyl ethers like vinyl acetate, which find broad applications in the paper, tex-

Table 1: Purity and yield of OXCART and OXOCART synthesized in various non-VOC solvents)

CTA	One-Pot Solvent	Yield (%)	Purity (%)
OXCART	DES	96	95
	TBAC	93	93
	COGE	64	60
	GTE	51	22
	EDGE	45	5.6
OXOCART	DES	94	94

tile, and pharmaceutical industries. Our manufacturing approach employs green solvents as organic media that merge seamlessly with the final product, eliminating the need for separation and representing a major advancement towards environmentally friendly chemical processes (Figure 2b, S2 and S3). To further assess the versatility of the methodology, we also explore the synthesis of OXCART/OXOCART in glycidyl-functional solvents in which competitive side reactions may be problematic.

2. Results and Discussion

The three classes of green solvents explored for this work included diethyl succinate (DES), tributyl acetyl citrate (TBAC), and the glycidyl ethers: glycerol triglycidyl ether (GTE), ethylene glycol diglycidyl ether (EDGE), and castor oil diglycidyl ether (COGE). The selection of these solvents was guided by the considerations of their commercial availability, cost-effectiveness, and reactivity with diverse nucleophiles under varying reaction conditions. In particular, epoxy-based solvents were chosen for their potential utility in polymerization reactions, leveraging their functional groups to improve compatibility within polymeric blends.

We synthesized OXCART following the procedure outlined by Cochran et al., with the replacement of acetone in the deprotonation step of ethanethiol, to green non-VOC solvents, as depicted in Figure 2b [29]. This addition enhances the reactivity between carbotrithioate salts and alkylating agents while also reducing solvent-related side reactions. The qualitative analysis of our synthesis revealed that citrate and ester-based solvents exhibited no significant physical differences compared to the Cochran et al. approach. In contrast, the use of epoxy-based solvents resulted in noticeable physical aberrations, including changes in coloration and the onset of exotherms due to competitive thiol-epoxy side reactions. Figures S6–S9 show the corresponding ^{1}H-NMR and ^{13}C-NMR spectra, confirming the formation of OXCART in both epoxy and citrate-based solvents. However, the purity and yield of CTA synthesized in epoxy-based solvents are diminished, as outlined in Table 1. A closer examination of the NMR spectra shows a loss of oxirane moiety (δ=2.2–2.7 ppm), indicating interactions between

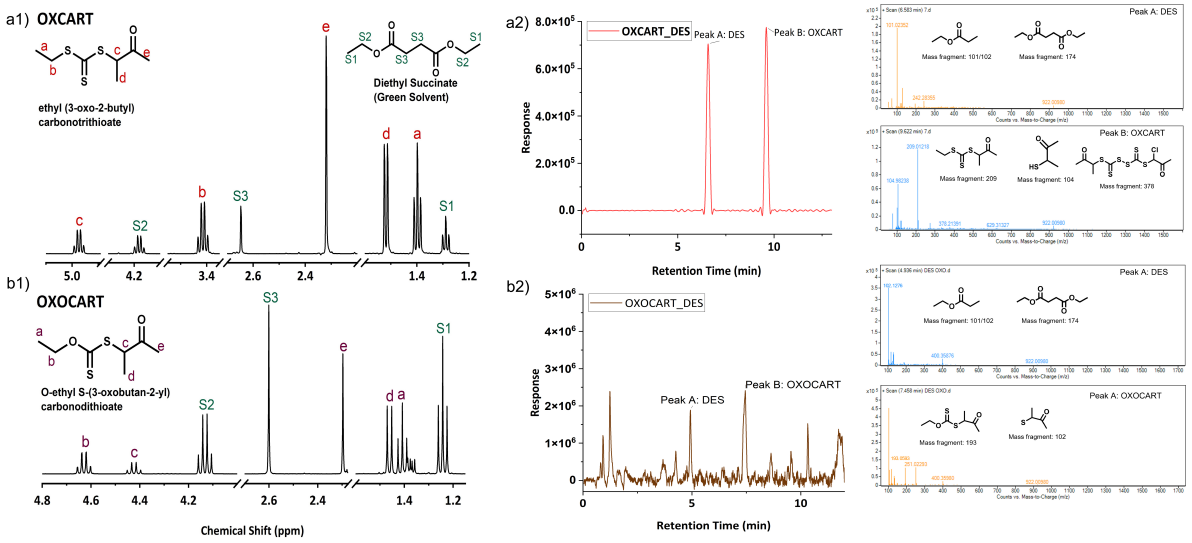

Figure 3: ^{1}H NMR spectra of OXCART and OXOCART synthesized using diethyl succinate (DES) as non-VOC solvent

the oxirane rings and the alkaline media. These interactions lead to the depletion of carbotrithioate intermediates, adversely affecting the product yield. This observation was further validated by LC-MS analysis (Figures S12–S17), which demonstrated significant variations in CTA purity based on solvent functionality. The CTA purity values remained > 90 % for inert DES and TBAC and dropped to 5-60 % for epoxy solvents, as indicated in Table 1. The wide CTA purity range for epoxy solvents can be attributed to their net epoxy equivalent weight (EEW) and epoxy values. Notably, EDGE and GTE exhibited the lowest product purity due to their short hydrocarbon chains, resulting in higher epoxy values that facilitated unintended reactions with active nucleophiles. In contrast, COGE demonstrated improved product purity due to its higher epoxy equivalent weight and lower epoxy value, which minimized solvent interactions with carbotrithioate salts. Furthermore, the LC-MS spectra of these one-pot CTAs made in epoxy-based solvents also revealed partial solvent oligomerization during the reaction. The highly nucleophilic environment led to partial ring-opening of epoxies, forming alcohol end groups that initiated oligomerization, increasing the reaction mixture's viscosity and hindering mass transfer between the reactants. This resulted in reduced purity and yield of the product. Specifically, for solvents like GTE and EDGE, this behavior can also be linked to the presence of a mixture of mono, di, and tri-glycidyl functional solvent molecules, which further accelerated oligomerization and by-product formation, as indicated by the large mass fragments detected in the mass spectra.

DES, in particular, emerged as the optimal solvent for synthesizing both OXCART and its xanthate variant (OXOCART). Distinct peaks for both the solvent and CTA were observed in the NMR and LC plots (Figure 3), indicating high CTA purity (Tables 1

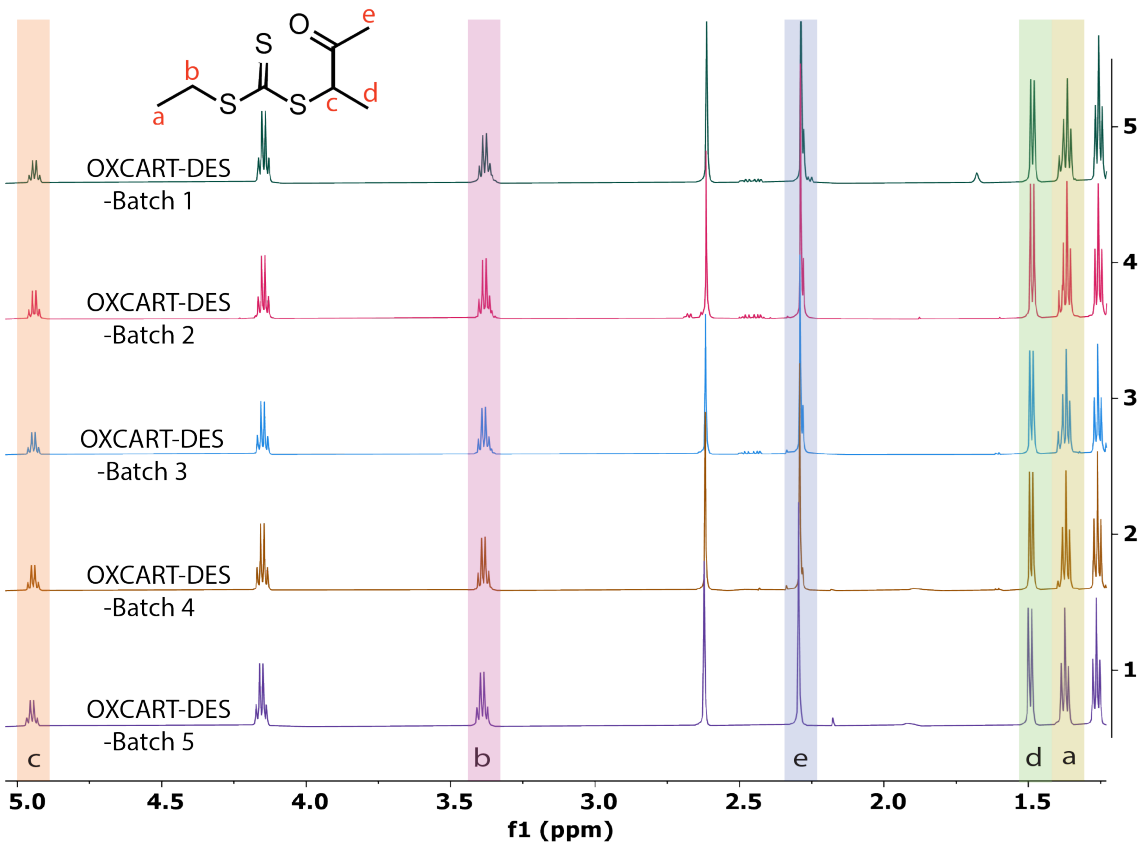

Figure 4: ^{1}H-NMR spectra comparison of OXCART synthesized in DES for different batches

and Table S3). This stability is due to the inert nature of ester linkages in DES toward nucleophiles at room temperature, unlike more reactive groups such as epoxies, preserving the integrity of both the solvent and CTA. A reproducibility study further supported this observation, where five batches of OXCART were synthesized in DES. Figure 4 and Table S5 depicts quantified data confirming consistent reproducibility across batches, with minimal variations and negligible formation of by-products. This consistency observed at the lab scale prompted us to scale the reaction to a 10L pilot volume (Figure S18). The reaction at 10L scale yielded results with comparable yield and purity to those observed at the laboratory scale. A quantitative NMR study, as depicted in Figure S21 and Table Table S7, confirms that consistent product purity was maintained across reaction scales ranging from 250 mL to 10 L. Additionally, we examined the temporal storage stability of these CTAs over a period of one year. NMR analysis (S20–S25 and Table Table S6–Table S11) showed that both CTAs when stored under standard refrigeration conditions (4°C), maintained high stability without decomposition or reactivity with the solvents.

These results demonstrate a successful scale-up of the CTA with consistent yields; however, it is essential to account for the biphasic nature of the reaction system. Inadequate mixing can cause severe exotherms, which can be managed by ensuring proper

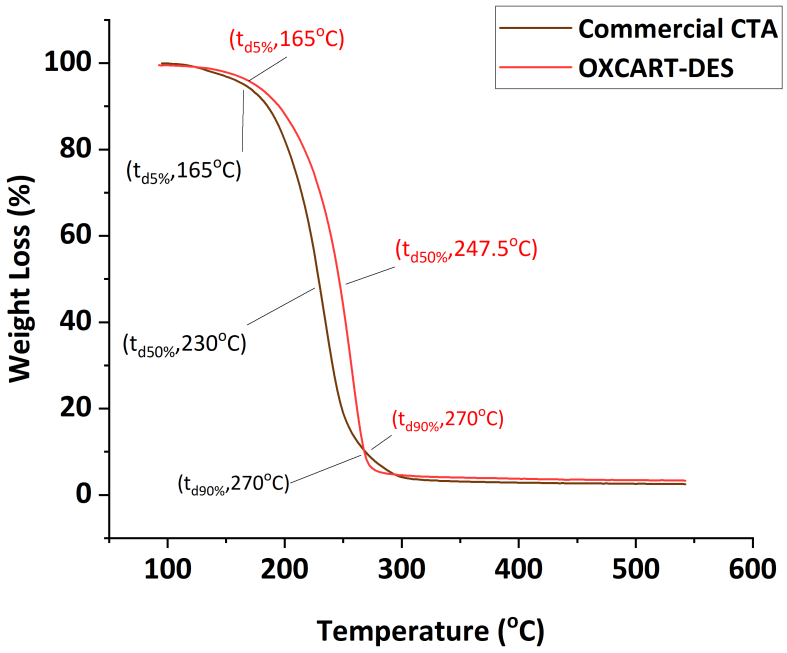

Figure 5: TGA thermogram showing the thermal stability comparison of commercially sold CTA and OXCART synthesized in a one-pot manner with DES as a solvent.

mixing and maintaining the reaction temperature at approximately 25°C with cooling coils. These precautions are crucial for both the safety and integrity of the synthesis process [30]. Furthermore, the thiocarbonylthio group present in the RAFT agent is sensitive to temperature and prone to thermal decomposition, making a thorough thermal decomposition study vital. Figure 5 presents the thermogravimetric analysis (TGA) of a commercially available CTA (2-cyanopropan-2-yl ethyl carbonotrithioate) compared to our one-pot synthesized CTA. Both CTAs exhibit single-stage decomposition in their TGA curves, while degrading uniformly within a narrow temperature range (165–270°C). This single-stage decomposition indicates a high thermal stability, with no significant intermediate degradation products. Nearly identical thermal decomposition rates between our CTA and the commercial agent underscore that the one-pot synthesis method using non-VOC solvents maintains thermal stability comparable to RAFT agents sold commercially, thus making it a viable, scalable alternative. Further TGA analysis for OXCART synthesized in other functional solvents is provided in the SI (Figure S19 and S4). These results indicate that using bulkier solvents with high EEW right shifts the thermal decomposition temperature of the mixture, providing some intermittent stability and leading to a multi-stage decomposition.

Furthermore, we evaluated the efficacy of OXCART variants in managing the reversible activation-deactivation cycles of propagating radicals across a multitude of commercially used monomers such as acrylates, acrylamides, styrenics, methacry-

Table 2: OXCART and OXOCART mediated polymerization data of commercially used monomers

CTA	Monomer	One-Pot Solvent	CTA/I	Conversion (%)	M_{nTheo} (kDa)	M_{nSEC} (kDa)	Đ
OXCART	MA	DES	8.05	93	11.0	11.1	1.03
		TBAC	8.45	94	11.1	11.4	1.03
		COGE	10.5	87	10.4	11.4	1.03
		GTE	20.0	90	10.8	11.1	1.06
		EDGE	27.5	40	4.9	8.7	1.09
	BA	DES	8.05	91	11.0	10.4	1.03
		TBAC	8.45	94	11.4	10.8	1.03
		COGE	10.5	87	10.6	11.2	1.04
		GTE	20.0	90	10.9	16.6	1.10
		EDGE	27.5	67	8.2	13.0	1.11
	DMA	DES	8.05	95	7.4	8.2	1.07
		TBAC	8.45	97	7.6	8.5	1.08
		COGE	10.5	93	7.2	9.1	1.10
		GTE	20.0	93	7.2	9.0	1.09
		EDGE	27.5	84	6.9	10.0	1.08
	Sty	DES	4.03	80	9.5	10.9	1.09
		TBAC	4.23	81	9.6	11.4	1.11
		COGE	5.25	81	9.6	12.7	1.11
		GTE	10.0	78	9.3	11.7	1.10
		EDGE	13.7	75	9.2	15.3	1.16
	MMA	DES	8.05	60	7.1	93.2	1.62
OXOCART	MA	DES	10.4	72	10.7	11.6	1.31
	BA	DES	10.4	78	10.6	10.8	1.28
	DMA	DES	10.4	92	7.0	6.7	1.13
	Sty	DES	5.20	74	9.3	13.5	1.40
	VAC	DES	10.4	65	7.9	7.9	1.13
	MMA	DES	10.4	58	6.9	70.9	1.94

(Abbreviations* DES: Diethyl Succinate, TBAC: Tributyl Acetyl Citrate, COGE: Castor Oil Diglycidyl Ether, GTE: Glycerol Triglycidyl Ether, EDGE: Ethylene Glycol Diglycidyl Ether, MA: Methyl Acrylate, BA: Butyl Acrylate, DMA: N,N Dimethyl Acrylamide, Sty: Styrene, Vac: Vinyl Acetate)
MMA: Methyl Methacrylate, uncontrolled polymerization with both CTAs)

lates, and vinyl esters. The polymerization for all monomers was initiated using 2,2'-azobis(2-methylpropionitrile) (AMBN) except for styrene, where dicumyl peroxide (DCP) was used. The CTA/I(initiator) ratio in these reactions was adjusted according to the concentration and impurity factors involved with each variant. Table 2 summarizes the degree of RAFT control exerted by different OXCART variants. The acrylates, acrylamide, and styrene showed great control (low Đ < 1.1) with high conversion for all OXCART types, except for OXCART-EDGE, which exhibited slight deviations in $M_{n,theo}$ values compared to $M_{n,SEC}$, as well as low conversion and bimodality (Figure S27). These anomalies can be attributed to the impurities (chain-terminating alcohols and bulky thiocarbonyl compounds) present in the CTA solution (confirmed via LC-MS

spectra), which act as terminating chain transfer units. Moreover, the low purity of OXCART-EDGE limits the access of active CTA to the polymeric chains, which inhibits their ability to attain RAFT equilibrium. However, it is worth noting that most of these one-pot CTAs have minimal impact on the polymerization process, highlighting their feasibility for usage in various end-use applications. DES and TBAC, for example, are valuable additives in pressure-sensitive adhesives, improving flexibility and tack. DES enhances adhesion and workability by lowering the adhesive's glass transition temperature, while tributyl acetyl citrate offers non-toxic plasticization and maintains adhesive performance across a broad temperature range [31, 32]. Epoxy-based solvents, on the other hand, play a crucial role in polymeric formulations by acting as reactive agents that enhance polymer adhesion, enable chain extension, and improve overall compatibility and processing [33]. Although these formulations were carried out in solution-based polymerizations, they may prove to be equally effective in emulsion-based polymerizations with proper tuning of the amphiphilic character of the CTAs. An exemplar system would involve the synthesis of poly(acrylic acid)–based oligomers as a macroCTA [34].

In general, trithiocarbonates (TTCs) are known to exhibit a high k_{add} (rate coefficient of monomer addition to CTA), in their interactions with propagating radicals, rendering them effective for precise control over "more-activated monomers" (MAMs), which are characterized by low k_{add} and k_{p} rates [35]. The OXCART structure used in the study has an R-group configuration that results in the formation of a secondary radical upon fragmentation. It provides the requisite transfer coefficient to the CTA, primarily owing to the carbonyl's tendency in the R-group to stabilize the radical more effectively than the propagating chain, facilitating greater fragmentation and stability of the intermediate adduct. This design, as shown in the proof of concept study, confers exceptional control over MAMs, which are all secondary propagating radical-based monomers. However, this control does not extend to methacrylates, which are tertiary propagating radicals; these monomers preferentially fragment upon interaction with the CTA, forming a more stable radical that undermines the CTA's control capabilities (Figure S28 & Table 2) [36]. Moreover, vinyl esters, classified as "low-activated monomers" (LAMs) with higher k_{add} and k_{p}, do not polymerize using OXCART, as indicated by NMR spectra after 8 hours of reaction (Figure S29). This lack of polymerization results from excessive chain-transfer events between the propagating radicals and the CTA, causing an infinite loop without further double-bond attacks (Figure S30). In contrast, OXOCART-DES exhibited precise molecular weight control during vinyl acetate polymerization, but only partial control with MAMs due to the low k_{add} of xanthates, which hinders the immediate attack of MAMs' propagating radicals on the thiocarbonylthio double bond in the xanthates. However, in some cases, this bond

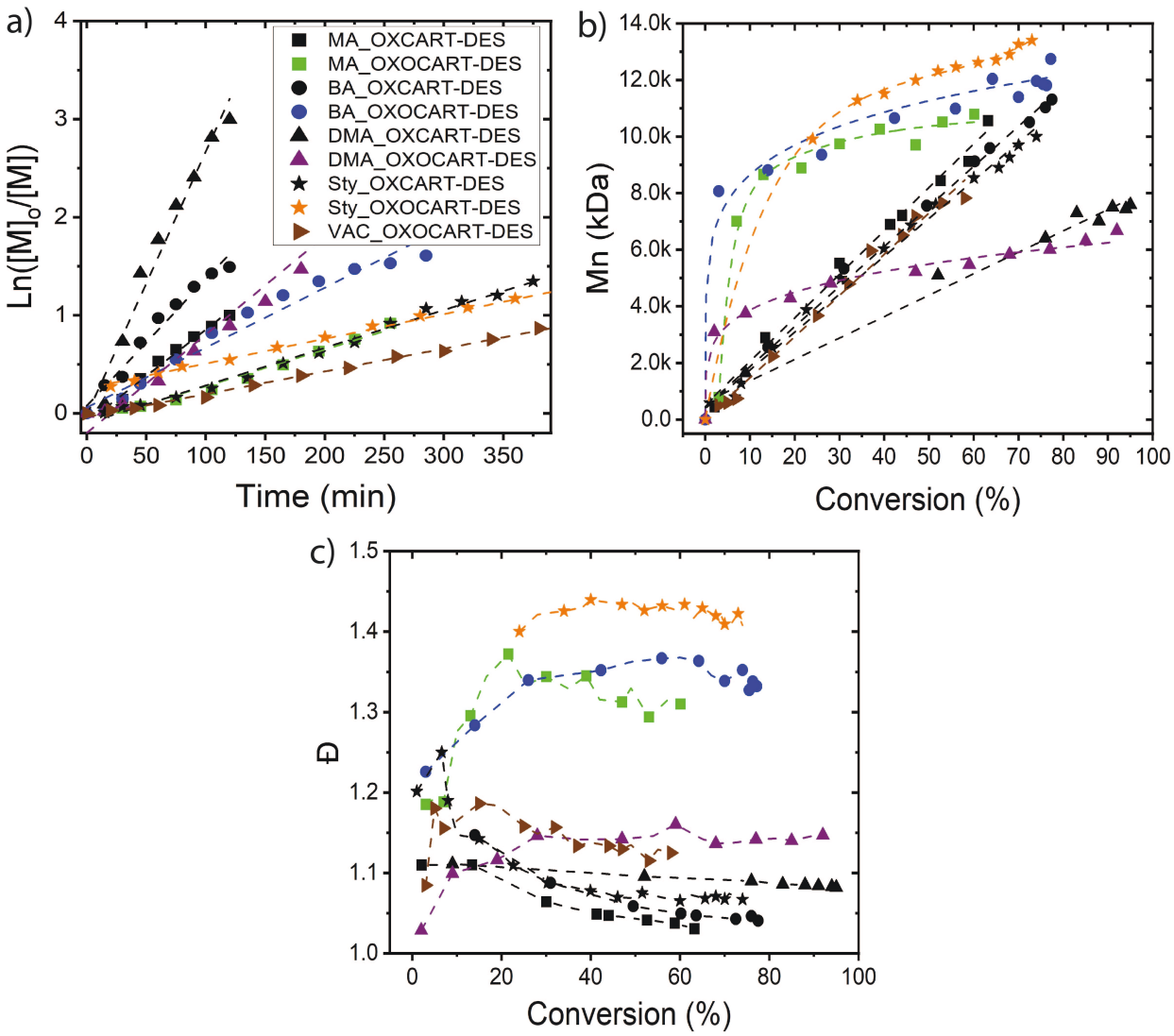

Figure 6: Kinetic study comparison of MAMs and LAMs polymerized with OXCART-DES and OXOCART-DES. a) Pseudo-first-order kinetics plot of the monomer conversion with respect to time (b) Molecular weight vs Conversion (c) Dispersity evolution of polymers w.r.t to conversion(Abbreviations: MA - Methyl Acrylate; BA - Butyl Acrylate; DMA - N,N Dimethyl Acrylamide; Sty - Styrene; VAC - Vinyl Acetate)

is attacked slowly, resulting in the partial control observed (Figure S31 & Table 2). To further assess the extent of RAFT control, we synthesized polymers targeting molecular weights of 100 kDa and 120 kDa (Figure S32). We observed a noticeable loss of RAFT control at these higher molecular weights owing to the exponential increase in viscosity at high conversions. Under such mass transfer limited viscous conditions, the RAFT agent's ability to effectively mediate the polymerization diminishes, resulting in a loss of control over the polymerization process [15].

We further conducted kinetic studies on these monomers with both CTAs to determine the presence of RAFT control during the polymerization process. Figure 6a illustrates the kinetic comparison between TTC and xanthate CTAs for MAMs, where OXCART-DES exhibited a linear pseudo-first-order correlation over time, indicating

a continuous radical supply during polymerization. Additionally, Figure 6b demonstrates a linear relationship between molecular weight and conversion, corroborated by Đ (Figure 6c) values close to 1, signifying the successful induction of living characteristics in polymerization. [29] Conversely, for OXOCART-DES, all monomers showed marked rate retardation, as evidenced by a sudden increase in M_n at intermediate conversion, plateauing at higher conversion levels. Dispersity values also indicated the induction of partial living characteristics. This retardation in MAMs can be attributed to two mechanisms: premature polymeric chain termination due to slow radical addition to the CTA, hindering further growth and broadening molecular weight distribution, and consumption of RAFT adducts due to their inherent instability, which explains the slower reaction rate and reduced conversion. In contrast, kinetic studies (Figure 6a) for LAMs with OXOCART-DES demonstrated pseudo-first-order kinetics and a linear M_n versus conversion trend, confirming the maintenance of RAFT equilibrium throughout the reaction. This stability is crucial for controlling LAMs, whose propagating radicals are unstable and characterized by high k_p and k_{add}. A less activated CTA effectively maintains control over oligomeric chain growth, preventing them from entering an excessive chain transfer cycle.

Furthermore, to demonstrate the livingness of the RAFT process using theis one-pot CTA, we synthesized a block copolymer containing a 20% initial soft marcroCTA and 80% hard block. Figure S33 illustrates that the unpurified one-pot homopolymer effectively facilitated the growth of the additional block, demonstrating the living character of these RAFT agents. The key feature of a living polymerization system like RAFT is its ability to maintain control over chain growth throughout the reaction. In our case, the successful extension of the polymeric chain from the macroCTA confirms that the RAFT agents retained their functionality, effectively controlling polymerization and allowing the formation of well-defined block copolymers.

3. Conclusion

This study has demonstrated that our method for synthesizing chain transfer agents (CTAs) is both facile and scalable, achieving high purity and yield. This success is attributed to the use of a non-VOC solvent that provides a non-reactive organic medium for both CTA synthesis and the polymerization process. A key advantage of our method over traditional CTA synthesis protocols is the elimination of energy-intensive separation processes to remove VOC solvents, enhancing accessibility, reducing costs, and simplifying use.

The effectiveness of these CTAs has been validated through polymerization and kinetics studies on various commercially significant monomers, confirming their capability to control RAFT equilibrium and maintain precise polymer molecular weights.

The dispersity values observed in our studies are comparable to those expected in living polymerization, highlighting the high chain transfer coefficient of the CTAs, which remains unaffected by the solvent. Importantly, the scalability of this method facilitates straightforward, large-scale production of functionalized polymers without the need for new production techniques.

This CTA manufacturing methodology could drastically improve the availability and economics of CTAs, helping RAFT to achieve its potential for precisely tailored polymer architectures in commercial practice. Looking ahead, our focus is directed towards developing scalable synthesis processes for CTAs that control methacrylates (tertiary radical-based), a major part of industrial polymer production. Simultaneously, the success of this approach opens avenues for exploring diverse polymeric architectures using bio-derived sources, making scalable functional polymer production easy.

4. Acknowledgement

We acknowledge the Iowa State University W.M. Keck Metabolomics Research Laboratory (RRID: SCR_017911) for providing analytical instrumentation and input for our LC-MS samples. We sincerely thank Dr Lucas J Showman for his assistance and support. Finally, we acknowledge the USDA Bioproduct Pilot Program (USDA #2022-09368) for financial support.

References

[1] J. Wu, L. Zhang, Y. Chen, J. Tan, J. Wu, L. Zhang, Y. Chen, J. Tan, Linear and star block copolymer nanoparticles prepared by heterogeneous raft polymerization using an ω,ω-heterodifunctional macro-raft agent, ACS Macro Letters (2022). doi:10.1021/ACSMACROLETT.2C00314.

[2] V. A. Ganesh, A. Baji, S. Ramakrishna, Smart functional polymers – a new route towards creating a sustainable environment, RSC Adv. 4 (95) (2014) 53352–53364. doi:10.1039/C4RA10631H.
URL http://xlink.rsc.org/?DOI=C4RA10631H

[3] A. Kumari, I. Pani, M. U. Lone, A. Aggarwal, S. K. Pal, R. K. Roy, Architectural Effect on Self-Assembly and Biorecognition of Randomly Grafted Linear and Branched Polymers at Liquid Crystal–Water Interfaces, ACS Applied Materials & Interfaces 15 (26) (2023) 31233–31242. doi:10.1021/acsami.3c04672.
URL https://pubs.acs.org/doi/10.1021/acsami.3c04672

[4] Y. EL-Ghoul, F. M. Alminderej, F. M. Alsubaie, R. Alrasheed, N. H. Almousa, Recent Advances in Functional Polymer Materials for Energy, Water, and Biomedical Applications: A Review, Polymers 13 (24) (2021) 4327. doi:10.3390/polym13244327.
URL https://www.mdpi.com/2073-4360/13/24/4327

[5] B. Zhao, J. Li, X. Yang, S. He, X. Pan, J. Zhu, Degradable 3D Printed Objects with Tunable Mechanical Properties *via* Photoinduced Free Radical Promoted Cationic RAFT Polymerization, ACS Applied Polymer Materials 6 (2) (2024) 1584–1591. doi:10.1021/acsapm.3c03164.
URL https://pubs.acs.org/doi/10.1021/acsapm.3c03164

[6] C. M. Bates, F. S. Bates, *50th Anniversary Perspective* : Block Polymers—Pure Potential, Macromolecules 50 (1) (2017) 3–22. doi:10.1021/acs.macromol.6b02355.
URL https://pubs.acs.org/doi/10.1021/acs.macromol.6b02355

[7] D. Baskaran, Strategic developments in living anionic polymerization of alkyl (meth)acrylates, Progress in Polymer Science 28 (4) (2003) 521–581. doi:10.1016/S0079-6700(02)00083-7.
URL https://linkinghub.elsevier.com/retrieve/pii/S0079670002000837

[8] H. Fouilloux, C. M. Thomas, Production and Polymerization of Biobased Acrylates and Analogs, Macromolecular Rapid Communications 42 (3) (2021) 2000530. doi:10.1002/marc.202000530.
URL https://onlinelibrary.wiley.com/doi/10.1002/marc.202000530

[9] C. Veith, F. Diot-Néant, S. A. Miller, F. Allais, Synthesis and polymerization of bio-based acrylates: a review, Polymer Chemistry 11 (47) (2020) 7452–7470. doi:10.1039/D0PY01222J.
URL http://xlink.rsc.org/?DOI=D0PY01222J

[10] A. Llevot, P. Dannecker, M. von□Czapiewski, L. C. Over, Z. Söyler, M. A. R. Meier, Renewability is not Enough: Recent Advances in the Sustainable Synthesis of Biomass-Derived Monomers and Polymers, Chemistry – A European Journal 22 (33) (2016) 11510–11521. doi:10.1002/chem.201602068.
URL https://chemistry-europe.onlinelibrary.wiley.com/doi/10.1002/chem.201602068

[11] F.-Y. Lin, A. D. Hohmann, N. Hernández, L. Shen, H. Dietrich, E. W. Cochran, Self-Assembly of Poly(styrene- *block* -acrylated epoxidized soybean oil) Star-Brush-Like Block Copolymers, Macromolecules 53 (18) (2020) 8095–8107. doi:10.

1021/acs.macromol.0c00441.
URL https://pubs.acs.org/doi/10.1021/acs.macromol.0c00441

[12] B. W. Kuehl, A. Hohmann, T. H. Lee, M. Forrester, N. Hernandez, H. Dietrich, C. Smith, S. Musselman, G. Tran, E. W. Cochran, Cavitation-Mediated Fracture Energy Dissipation in Polylactide at Rubbery Soybean Oil-Based Block Copolymer Interfaces Formed via Reactive Extrusion, ACS Applied Materials & Interfaces 14 (41) (2022) 46912–46919. doi:10.1021/acsami.2c10496.
URL https://pubs.acs.org/doi/10.1021/acsami.2c10496

[13] W. A. Braunecker, K. Matyjaszewski, Controlled/living radical polymerization: Features, developments, and perspectives, Progress in Polymer Science 32 (1) (2007) 93–146. doi:10.1016/j.progpolymsci.2006.11.002.
URL https://linkinghub.elsevier.com/retrieve/pii/S007967000600133X

[14] N. Corrigan, K. Jung, G. Moad, C. J. Hawker, K. Matyjaszewski, C. Boyer, Reversible-deactivation radical polymerization (controlled/living radical polymerization): From discovery to materials design and applications, Progress in Polymer Science (2020). doi:10.1016/J.PROGPOLYMSCI.2020.101311.

[15] S. Perrier, *50th Anniversary Perspective* : RAFT Polymerization—A User Guide, Macromolecules 50 (19) (2017) 7433–7447. doi:10.1021/acs.macromol.7b00767.
URL https://pubs.acs.org/doi/10.1021/acs.macromol.7b00767

[16] C. Boyer, V. Bulmus, T. P. Davis, V. Ladmiral, J. Liu, S. Perrier, Bioapplications of raft polymerization., Chemical Reviews (2009). doi:10.1021/CR9001403.

[17] C. Boyer, M. Stenzel, T. P. Davis, Building nanostructures using raft polymerization, Journal of Polymer Science: Part A (2011). doi:10.1002/POLA.24482.

[18] G. Moad, Raft polymerization to form stimuli-responsive polymers, Polymer Chemistry 8 (2017) 177–219. doi:10.1039/C6PY01849A.

[19] G. Moad, R. Mayadunne, E. Rizzardo, M. Skidmore, S. Thang, Synthesis of novel architectures by radical polymerization with reversible addition fragmentation chain transfer (raft polymerization), Macromolecular Symposia 192 (2003) 1–12. doi:10.1002/MASY.200390029.

[20] J. Sun, C. Wang, Y. Hong, Z.-W. Tan, C. Liu, Phosphine oxide-containing multifunctional polymer via raft polymerization and its high-density post-polymerization modification in water, ACS Applied Polymer Materials 3 (2021) 3214–3226. doi:10.1021/ACSAPM.1C00403.

[21] F. Faghihi, P. Hazendonk, Raft polymerization, characterization, and post-polymerization modification of a copolymer of vinylbenzyl chloride: Towards thiolate functionalized copolymers, Polymer (2017). doi:10.1016/J.POLYMER.2017.08.067.

[22] M. Yan, Y. Huang, M. Lu, F.-Y. Lin, N. Hernandez, E. W. Cochran, Gel point suppression in raft polymerization of pure acrylic cross-linker derived from soybean oil, Biomacromolecules (2016). doi:10.1021/ACS.BIOMAC.6B00745.

[23] M. Destarac, Controlled Radical Polymerization: Industrial Stakes, Obstacles and Achievements, Macromolecular Reaction Engineering 4 (3-4) (2010) 165–179. doi:10.1002/mren.200900087.
URL https://onlinelibrary.wiley.com/doi/10.1002/mren.200900087

[24] T. P. Le, G. Moad, E. Rizzardo, S. H. Thang, Polymerization with living characteristics, Patent number: WO1998001478A1 (1998).

[25] P. Corpart, D. Charmot, T. Biadatti, S. Zard, D. Michelet, Method for block polymer synthesis by controlled radical polymerisation, Patent number: WO1998058974A1 (1998).

[26] M. Destarac, Industrial development of reversible-deactivation radical polymerization: is the induction period over?, Polymer Chemistry (2018). doi:10.1039/C8PY00970H.

[27] J. Skey, R. K. O'Reilly, Facile one pot synthesis of a range of reversible addition–fragmentation chain transfer (RAFT) agents, Chemical Communications (35) (2008) 4183. doi:10.1039/b804260h.
URL http://xlink.rsc.org/?DOI=b804260h

[28] S. W. Spring, C. S. Cerione, J. H. Hsu, S. L. Shankel, B. P. Fors, Scalable, Green Chain Transfer Agent for Cationic RAFT Polymerizations, Chinese Journal of Chemistry 41 (4) (2023) 399–404. doi:10.1002/cjoc.202200557.
URL https://onlinelibrary.wiley.com/doi/10.1002/cjoc.202200557

[29] E. W. COCHRAN, N. HERNANDEZ, M. Forrester, A. Hohmann, Thiocarbonylthio compounds as chain transfer agents suitable for raft polymerization, Patent number: US-10968173-B2 (2019).

[30] F. Mandrelli, A. Buco, L. Piccioni, F. Renner, B. Guelat, B. Martin, B. Schenkel, F. Venturoni, The scale-up of continuous biphasic liquid/liquid reactions under super-heating conditions: methodology and reactor design, Green Chemistry

19 (6) (2017) 1425–1430. doi:10.1039/C6GC02840C.
URL https://xlink.rsc.org/?DOI=C6GC02840C

[31] A. Stuart, M. M. McCallum, D. Fan, D. J. LeCaptain, C. Y. Lee, D. K. Mohanty, Poly(vinyl chloride) plasticized with succinate esters: synthesis and characterization, Polymer Bulletin 65 (6) (2010) 589–598. doi:10.1007/s00289-010-0271-4.
URL http://link.springer.com/10.1007/s00289-010-0271-4

[32] V. Tanrattanakul, P. Bunkaew, Effect of different plasticizers on the properties of bio-based thermoplastic elastomer containing poly(lactic acid) and natural rubber, Express Polymer Letters 8 (6) (2014) 387–396. doi:10.3144/expresspolymlett.2014.43.
URL http://www.expresspolymlett.com/letolt.php?file=EPL-0005014&mi=c

[33] R. Venderbosch, H. Meijer, P. Lemstra, Processing of intractable polymers using reactive solvents: 3. Mechanical properties of poly(2,6-dimethyl-1,4-phenylene ether) processed by using various epoxy resin systems, Polymer 36 (15) (1995) 2903–2913. doi:10.1016/0032-3861(95)94339-U.
URL https://linkinghub.elsevier.com/retrieve/pii/003238619594339U

[34] S. Fréal-Saison, M. Save, C. Bui, B. Charleux, S. Magnet, Emulsifier-Free Controlled Free-Radical Emulsion Polymerization of Styrene via RAFT Using Dibenzyltrithiocarbonate as a Chain Transfer Agent and Acrylic Acid as an Ionogenic Comonomer: Batch and Spontaneous Phase Inversion Processes, Macromolecules 39 (25) (2006) 8632–8638. doi:10.1021/ma061572s.
URL https://pubs.acs.org/doi/10.1021/ma061572s

[35] D. J. Keddie, G. Moad, E. Rizzardo, S. H. Thang, RAFT Agent Design and Synthesis, Macromolecules 45 (13) (2012) 5321–5342. doi:10.1021/ma300410v.
URL https://pubs.acs.org/doi/10.1021/ma300410v

[36] A. Ilchev, R. Pfukwa, L. Hlalele, M. Smit, B. Klumperman, Improved control through a semi-batch process in RAFT-mediated polymerization utilizing relatively poor leaving groups, Polymer Chemistry 6 (46) (2015) 7945–7948. doi:10.1039/C5PY01293G.
URL http://xlink.rsc.org/?DOI=C5PY01293G

RAFT Unchained — Scalable Manufacturing Of Thiocarbonyl Chain Transfer Agents

Vivek Garg, Anna McCaslin, Michael Forrester, Baker Kuehl, Sharan Raman, Dhananjay Dileep, Eric Cochran

Electronic Supporting Information

Materials and Method

Materials

All monomers: Methyl acrylate (MA, 99%), Styrene (99%+), Vinyl acetate (VAC, 99%), N,N-dimethyl acrylamide (DMA, 99%), and methyl methacrylate (MMA, 99%) were procured from Sigma Aldrich and were used as purchased without further purification. Green Solvents: Diethyl succinate (DES, Sigma Aldrich), Tributyl O-acetyl citrate (TBAC, Sigma Aldrich), Ethylene glycol diglycidyl ether (EDGE, Sigma Aldrich), Castor oil diglycidyl ether (COGE, BOC Sciences), and Glycerol triglycidyl ether (GTE, Biosynth AG, Switzerland) were used as received. Ethanethiol (97%) was procured from Oakwood Products Inc. Carbon disulfide (99%) was purchased from Fischer Scientific. Ethanol, 3-chloro-2-butanone, 2,2'-Azobis(2-methylpropionitrile) (AMBN), Azobisisobutyronitrile (AIBN), and Dicumyl Peroxide (DP) were purchased from Sigma Aldrich with purities of 97% or higher.

All other solvents and reagents used throughout the experimentation were procured from either Sigma Aldrich or Fischer Scientific/Thermo Fischer Scientific.

Characterization/Instrumentation

Nuclear Magnetic Resonance (NMR) Spectra

Molecular structure and monomer conversion were assessed using a Bruker AVII 600 MHz proton nuclear magnetic resonance (^{1}H-NMR) spectrometer. D-chloroform served as the solvent for sample preparation, with Tetramethylsilane (TMS) employed as the internal standard unless stated otherwise. The NMR samples underwent 16 scans, with a 1-second delay time between scans.

Size Exclusion Chromatography (SEC)

Molecular weights and their distributions were recorded using a Waters Size Exclusion Chromatograph (SEC) equipped with an isocratic solvent manager (ACQ-ISM), UV detector (ACQ-UV), Refractive index detector (ACQ-RI), and five ethylene bridge hybrid (BEH) based packed columns connected in series (1x XT900A APC column (300,000-2,000,000), 1x XT450A APC column (20,000-400,000), 2x XT200A APC

(3,000-70,000) column, and 1x XT45A APC column (200-5,000)). The eluent used was Tetrahydrofuran (THF), maintained at a temperature of 25 °C, with a flow rate of 0.8 mL/min. The SEC system was calibrated with polystyrene (PS) and polymethyl methacrylate (PMMA) standards. The samples were prepared by dissolving 5 mg of polymer per 1 ml of THF and then filtered through a 0.45 µm PTFE filter before injection.

Liquid Chromatography-Mass spectrometry (LC-MS)

Approximately a 4 μL sample of each CTA sample was added and weighed into 2-mL LC-MS vial. The samples were diluted with 1.50 mL of LC-MS grade dilution solvent (1:1:1 LC-MS grade methanol : isopropanol : acetonitrile). The samples were further diluted 1:2 with dilution solvent before being subjected to LC-MS analysis. A high purity reference sample of (95.57% & 94.24%) TTC-CTA and Xan-CTA respectively (NMR, HPLC and LC-MS verified) were leveraged as a standard and a 1:1 serial dilutions was used to produce a calibration curve from 0.037 to 4.712 mg per sample. After sample preparation, the sample extracts were immediately subjected to LC-MS analysis.

LC separations were performed with an Agilent Technologies 1290 Infinity Binary Pump UHPLC instrument equipped with an Agilent Technologies Eclipse C8 1.8 µm 2.1 mm × 100 mm analytical column that was coupled to an Agilent Technologies 6540 UHD Accurate-Mass Q-TOF mass spectrometer (Agilent Technologies, Santa Clara, CA). A volume of 7 μL of each sample was injected into the LC system. Chromatography was carried out at 40 °C with a flow rate of 0.400 mL/min. Running solvents were A: water with 5 mM ammonium formate and 0.1% formic acid and B: 50% isopropanol in acetonitrile with 5 mM ammonium formate and 0.1% formic acid. Initial solvent conditions were 0% B which increased on a linear gradient to 100% B over 15-minutes, 100% B was held for 5-minutes before returning to 0% B over 2-minutes. A 6-minute post run at 0% B was conducted after each LC-MS acquisition.

Molecular features were detected using electrospray ionization in positive ionization mode. Nitrogen was used as the service gas for the ion source with a drying gas flow rate of 12 L/minute at a temperature of 350°C, a nebulizing pressure of 25 psi, and a sheath gas flow of 11 L/minute at 400 °C. The capillary and nozzle voltages were 4000 and 1750 volts respectively. The mass spectrometer was operated in high resolution (4Gz) mode with a scan range from m/z 100 to m/z 1700. An acquisition rate of 1.5 spectra per second was used. Reference masses were monitored for continuous mass calibration during LC-MS data acquisition: m/z 121.050873 with m/z 922.009698. UV-Vis data was collected in series with the MS, using an Agilent 1200 series DAD (diode array detector) (Agilent Technologies, Santa Clara, CA). Data

peak evaluation identifications were performed using Agilent MassHunter Qualitative Analysis (version 10.0, Agilent Technologies, Santa Clara, CA). The DAD signal at 313 nm was monitored for TTC-CTA and Xan-CTA purity and to assess for related side products and similar contaminants. While CTA quantification was accomplished using Agilent MassHunter Quantitative Analysis (version 10.0) software (Agilent Technologies, Santa Clara, CA). All the CTAs were quantified via extracted ion chromatogram (EIC) with a m/z of 209.0129 and a peak retention time of 9.60-minutes. Final purity calculations (% wt./wt.) were made relative to the reference sample linear standard curve, and solvent mass.

Thermogravimetric Analysis (TGA)

Thermogravimetric Analysis (TGA): The thermal decomposition of various one-pot RAFT agents was examined using a Netzsch STA449F1 thermogravimetric analyzer. The analysis employed a tungsten furnace capable of operating from room temperature up to 2400 °C, with a high sensitivity of 0.025 µg. The samples were heated from 40 °C to 600 °C at a rate of 10.0 °C min−1 while placed in aluminum pans. The data was processed using the Proteus® software. The purge gas consisted of a mixture of nitrogen, oxygen, and nitrogen, with respective intake flow rates of 10 ml min^{-1}, 10 mL min^{-1}, and 20 mL min^{-1}.

Methods

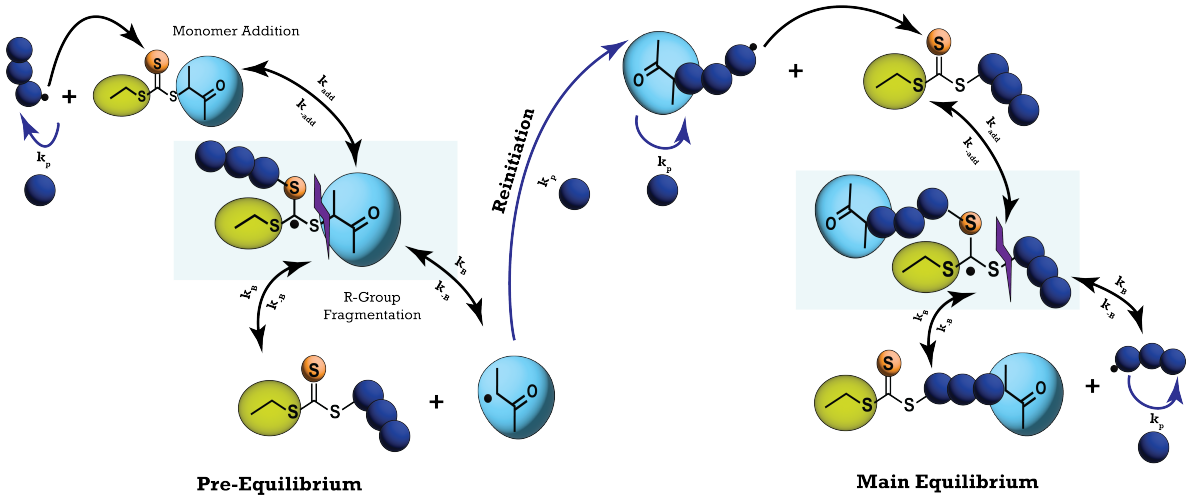

Scheme S1: Schematic representing reversible addition-fragmentation chain transfer polymerization using a trithiocarbonate as chain transferring agent

Synthesis of One-pot Ethyl (3-oxobutan-2-yl) carbonotrithioate (OXCART)

OXCART was synthesized using a single-step, one-pot addition approach. 8.84g (158 mmol) of potassium hydroxide (KOH) was added to a round bottom filled with deionized water (DI) and kept in a water/ice bath under constant stirring. Once the

KOH was dissolved, ethanethiol (8.94g, 144 mmol) was added dropwise to the flask, allowing it to stir for 30 minutes. Following this, 11.29g (148 mmol) of carbon disulfide was then added dropwise to the reaction mixture, maintaining the reaction temperature below 25 °C to give an orange-colored solution. Subsequently, a green solvent (DES, EDGE, GTE, TBAC, and COGE) and 3-chloro-2-butanone were added to the reaction mixture (1:1 molar ratio to ethanethiol), yielding a biphasic solution mixture: an organic layer consisting of green solvent and OXCART and an aqueous layer consisting of unreacted salts, and the organic layer was decanted to yield OXCART.

^{1}H NMR, δ (ppm from TMS): OXCART - 1.39-1.41 (3H's, -CH_2-CH_3), 3.38-3.42 (2H's, -S-CH_2-CH_3), 2.32 (3H's, -(O)C-CH_3), and 4.7-5.1 (3H's, O=C(CH_3)-S)
^{13}C NMR, δ (ppm from TMS): a - 12.76, b - 31.6, c - 222.12, d - 54.11, e - 15.21, f-204.18, g- 27.71

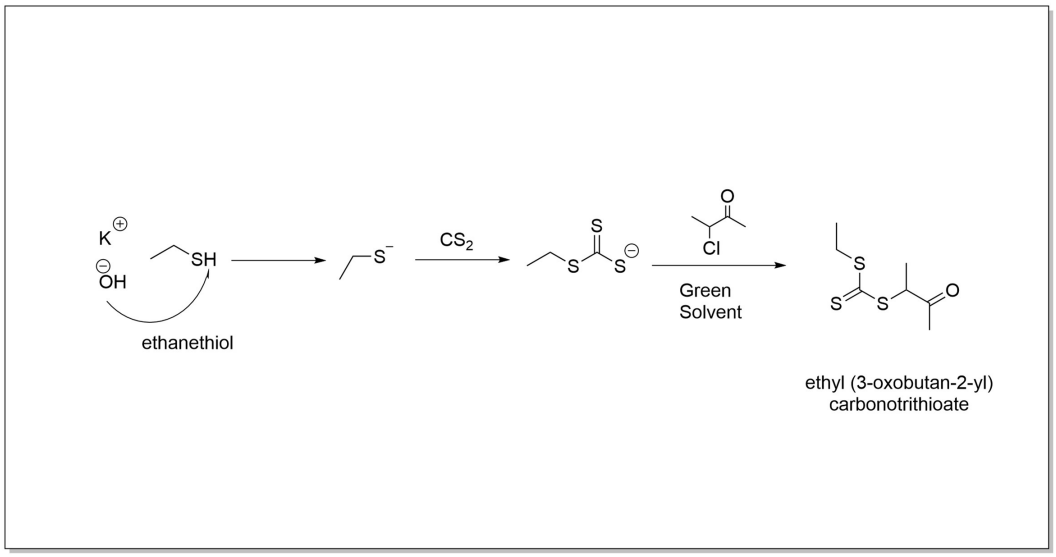

Scheme S2: Reaction mechanism for synthesizing OXCART

Synthesis of One-pot O-ethyl S-(3-oxobutan-2-yl) carbonodithioate (OXOCART)

OXOCART was synthesized using a comparable approach to the one used for OXCART. It included all 4-steps in a one-pot process, with the only variation being the substitution of ethanethiol with ethanol. Notably, the deprotonation step for ethanol necessitated a longer duration due to the higher bond strength of the hydrogen attached to oxygen in ethanol in contrast to the sulfur-hydrogen bond in a thiol.

^{1}H NMR, δ (ppm from TMS): OXOCART - 1.39-1.41 (3H's, -CH_2-CH_3), 3.38-3.42 (2H's, -S-CH_2-CH_3), 2.32 (3H's, -(O)C-CH_3), and 4.7-5.1 (3H's, O=C(CH_3)-S)
^{13}C NMR, δ (ppm from TMS): a - 13.67, b - 70.46, c - 212.53, d - 53.92, e - 15.45, f-204.46, g- 27.52

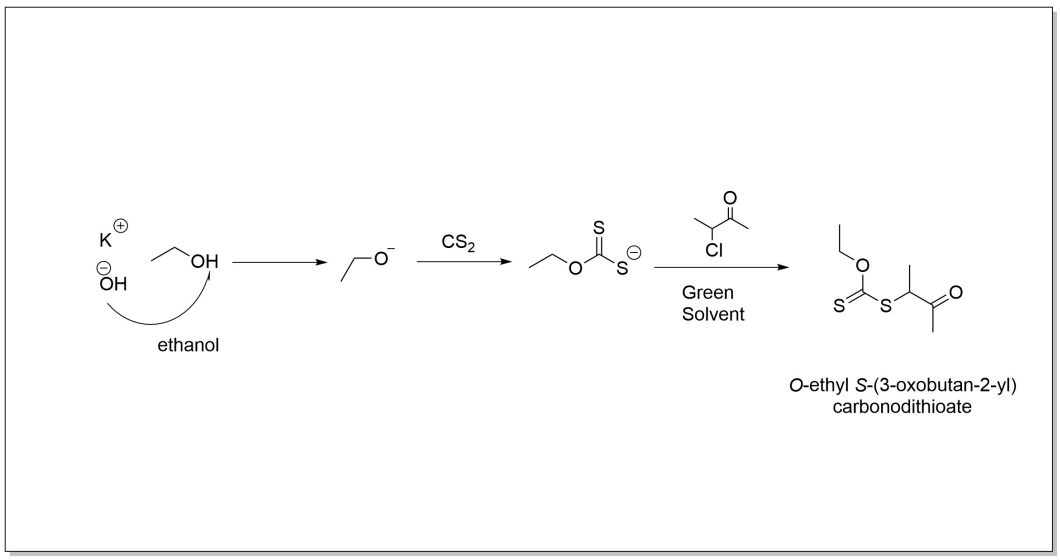

Scheme S3: Reaction mechanism for synthesizing OXOCART

RAFT polymerization of More Activated Monomers (MAM's) and Less Activated Monomers (LAM's)

Tables S1 and S2 (supplementary) provide the specific conditions for each polymerization performed. The appropriate reactants were added to a 3-necked round bottom flask equipped with a magnetic stirrer. The reaction mixture was subsequently sparged with Argon for 20-30 minutes to eliminate any unwanted contaminants. The solution mixture was then finally immersed in an oil bath, maintaining a specific temperature for the required polymerization duration. (All the monomers were polymerized using Toluene as a solvent except methyl methacrylate, also styrene was polymerized using dicumyl peroxide as the initiator).

In order to monitor the kinetics of the polymerization reaction, samples were extracted at predefined time intervals using a purging needle and a suction needle concurrently. The purging needle established an inert atmosphere while the suction needle was inserted into the flask to collect samples. The target molecular weight for all the polymerization reactions was 12.5 kDa. The percentage conversion of the monomer was assessed using ^{1}H NMR, and molecular weights along with the polydispersity index were determined through SEC analysis.

Table S1: RAFT polymerization conditions and composition for trithiocarbonate-based CTA (OXCART)

S.No	Monomer	One-Pot Solvent	Monomer amount (g)	CTA/I	Monomer conc. (g/ml)	Temperature (° C)	Time (hrs)
1	MA	DES	9	8.05	1	60	5
2	MA	TBAC	9	8.45	1	60	5
3	MA	COGE	9	10.5	1	60	5
4	MA	GTE	9	20.0	1	60	5
5	MA	EDGE	9	27.5	1	60	5
6	BA	DES	9	8.05	1	65	5
7	BA	TBAC	9	8.45	1	65	5
8	BA	COGE	9	10.5	1	65	5
9	BA	GTE	9	20.0	1	65	5
10	BA	EDGE	9	27.5	1	65	5
11	DMA	DES	5.5	8.00	3	65	4
12	DMA	TBAC	5.5	8.45	3	65	4
13	DMA	COGE	5.5	10.5	3	65	4
14	DMA	GTE	5.5	20.0	3	65	4
15	DMA	EDGE	5.5	27.5	3	65	4
16	STY	DES	9	4.03	1	120	8
17	STY	TBAC	9	4.23	1	120	8
18	STY	COGE	9	5.25	1	120	8
19	STY	GTE	9	10.0	1	120	8
20	STY	EDGE	9	13.8	1	120	8
21	MMA*	DES	9	8.05	1	80	5
22	VAC**	DES	9	8.05	1	70	8

(*Indicates conditions where polymerization was uncontrolled. ** Indicates polymerization conditions where polymerization did not occur.)

Table S2: RAFT polymerization conditions and composition for Xanthate-based CTA (OXOCART)

S.No	Monomer	One-Pot Solvent	Monomer amount (g)	CTA/I	Monomer conc. (g/ml)	Temperature (° C)	Time (hrs)
1	MA	DES	13	10.4	1	60	5
2	BA	DES	100	10.4	1	65	5
3	DMA	DES	5.5	10.4	1	65	4
4	STY	DES	9	5.20	1	120	8
5	MMA*	DES	9	10.4	1	80	5
6	VAC	DES	9	10.4	1	70	8

(*Indicates conditions where polymerization was uncontrolled.)

Table S3: LCMS data for OXCART and OXOCART synthesized in different green solvents

CTA	**RT (min)**	**Area (cm^2)**	**Calc. (%) Data**	**Mass (mg)**	**Purity (%) (%wt/wt)**
OXCART	9.60	1117	101.40	5	95
OXOCART	9.60	1108	100.70	5	94
OXCART-DES	9.59	900.5	81.89	5.5	95
OXOCART-DES	9.59	797.0	72.54	4.9	94
OXCART-TBAC	9.60	751.5	68.43	4.8	93
OXCART-COGE	9.60	467.2	42.76	4.0	60
OXCART-GTE	9.59	15.11	1.95	4.1	22
OXCART-EDGE	9.60	81.41	7.93	6.6	5.6

(* & DES: Diethyl Succinate, TBAC: Tributyl Acetyl Citrate, COGE: Castor Oil Diglycidyl Ether, GTE: Glycerol Triglycidyl Ether, EDGE: Ethylene Glycol Diglycidyl Ether)

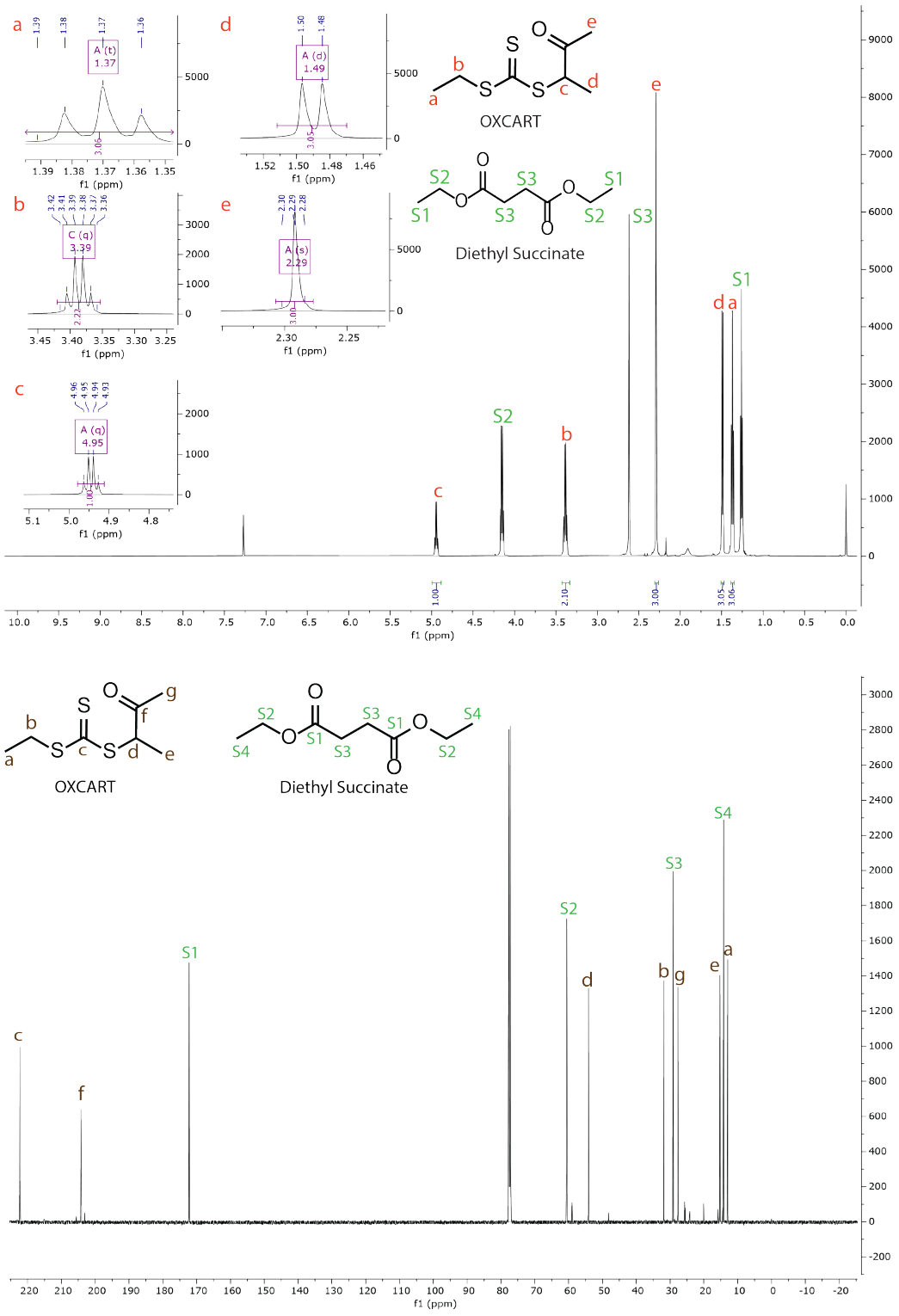

Figure S4: Complete ^{1}H-NMR and ^{13}C-NMR spectra of OXCART synthesized in DES as a one-pot solvent.

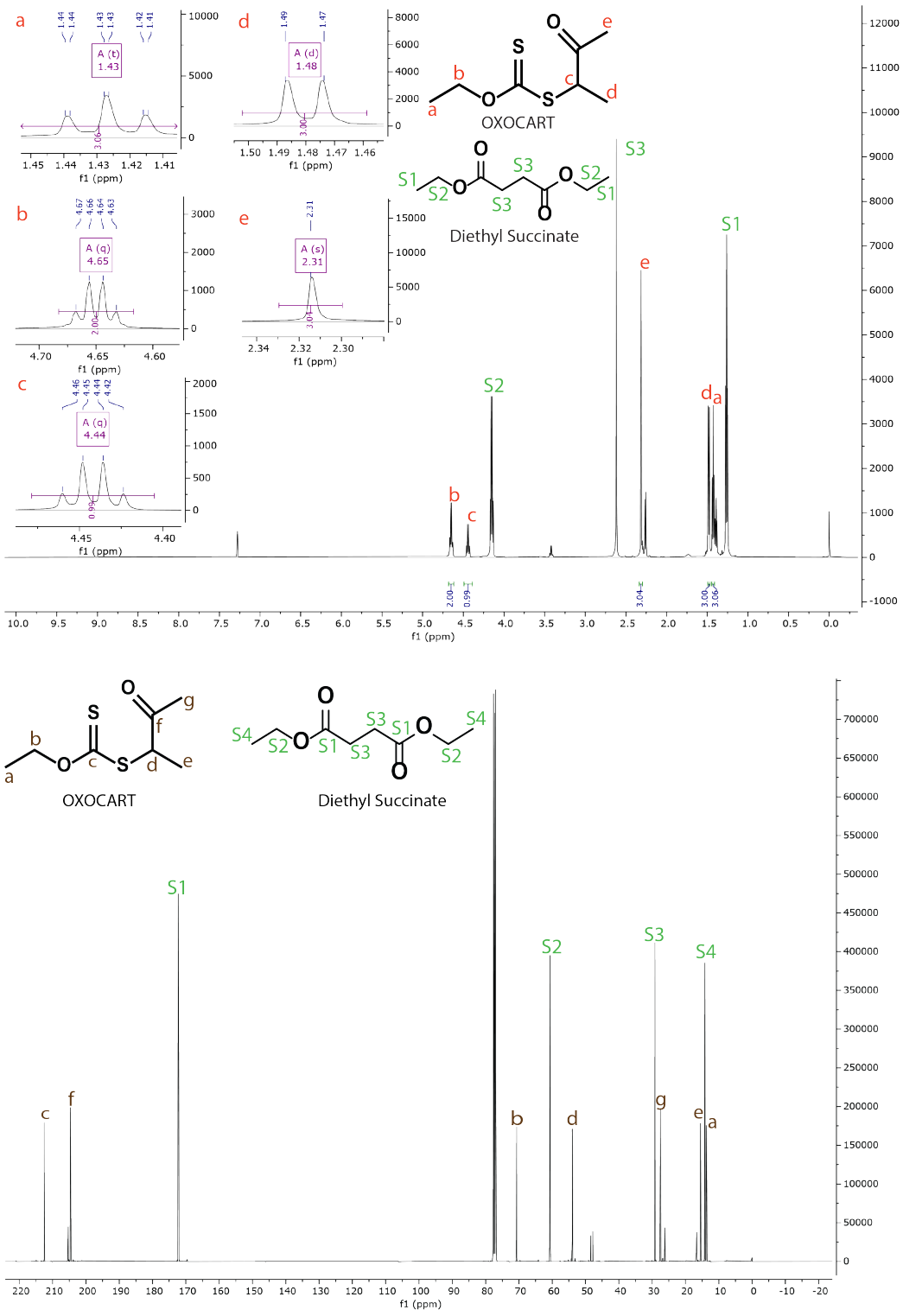

Figure S5: Complete ^{1}H NMR and ^{13}C-NMR spectra of OXOCART synthesized in DES as a one-pot solvent.

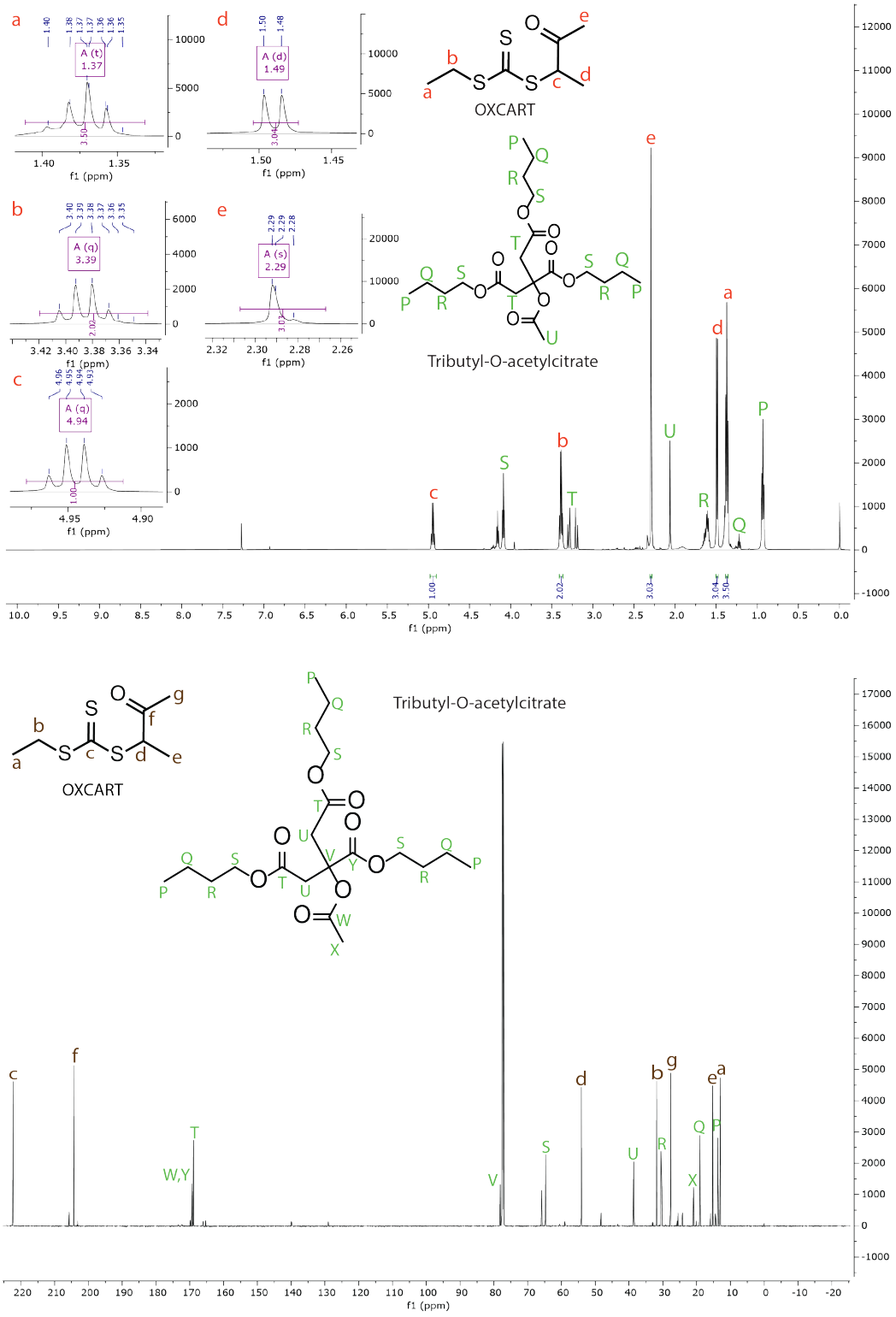

Figure S6: Complete ^{1}H NMR and ^{13}C-NMR spectra of OXCART synthesized in TBAC as a one-pot solvent.

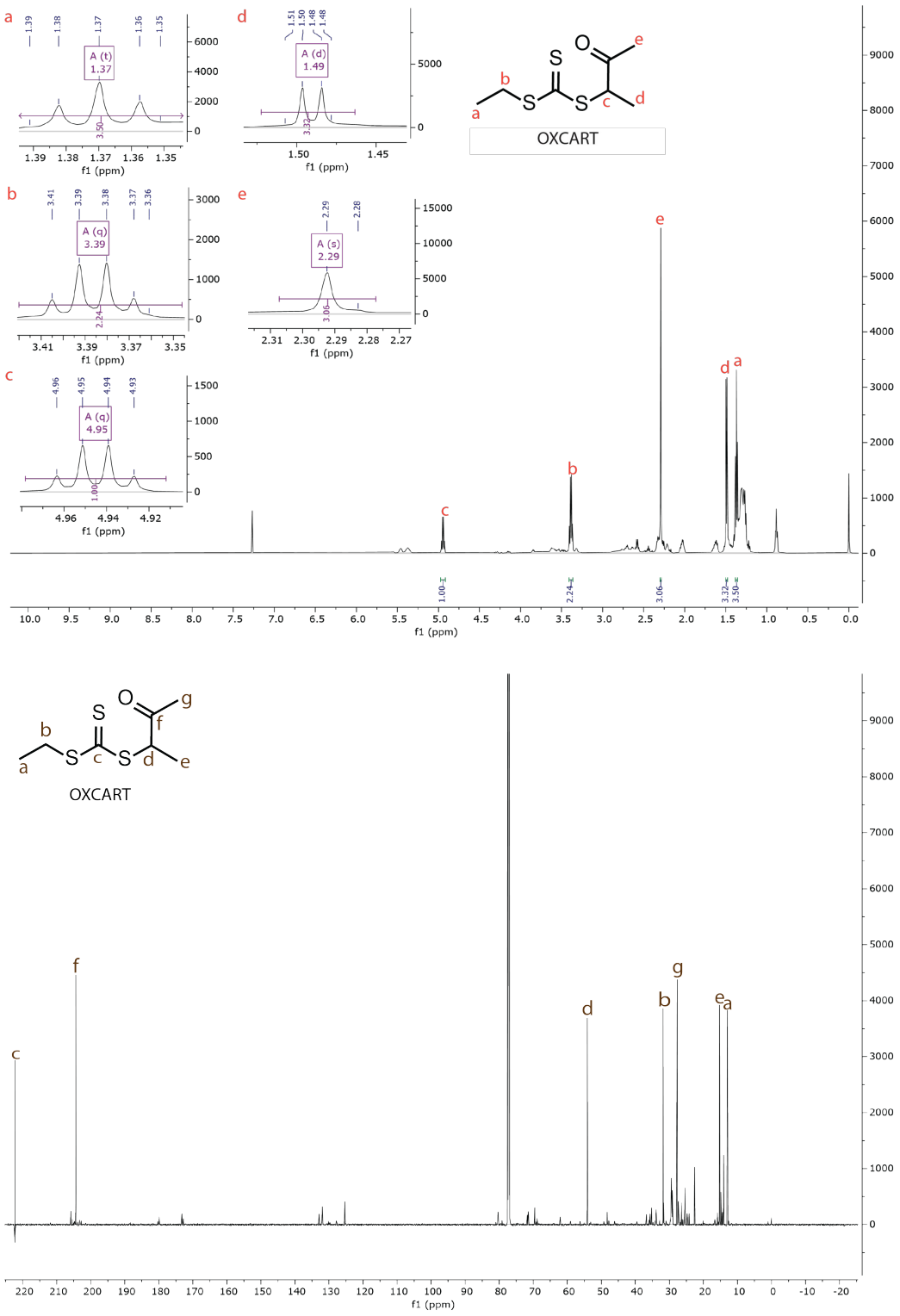

Figure S7: Complete ^{1}H NMR and ^{13}C-NMR spectra of OXCART synthesized in COGE as a one-pot solvent.

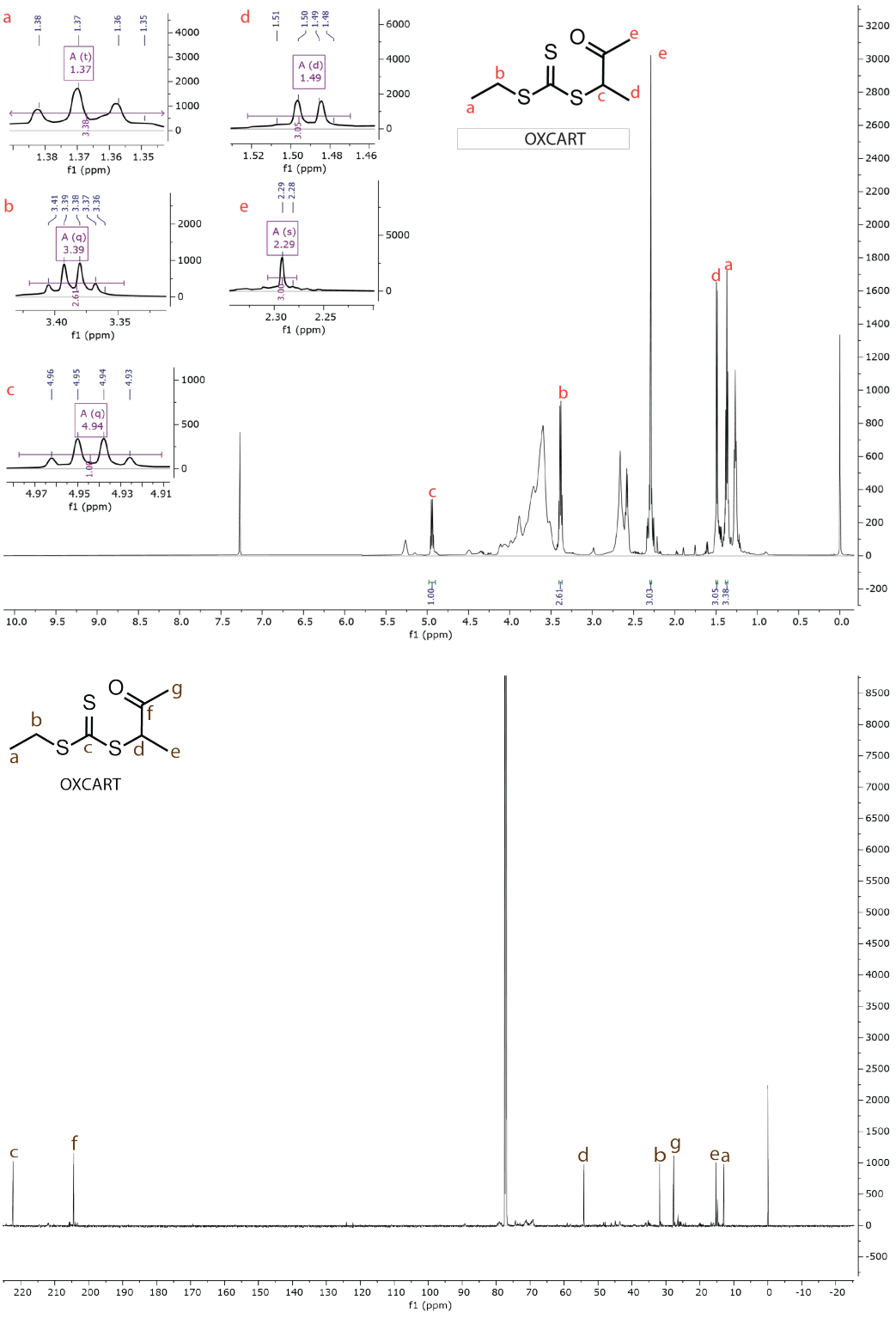

Figure S8: Complete ^{1}H NMR and ^{13}C NMR spectra of OXCART synthesized in GTE as a one-pot solvent.

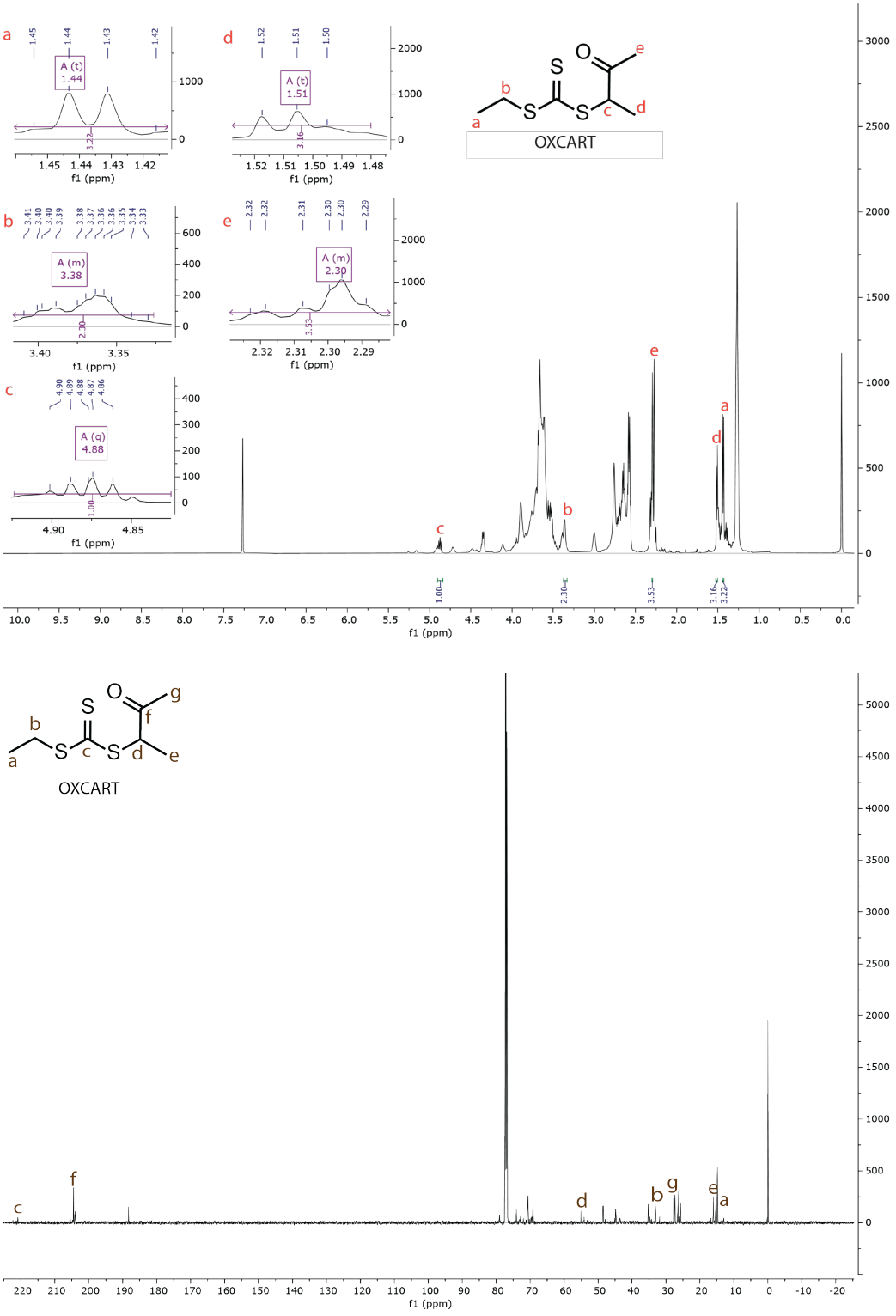

Figure S9: Complete ^{1}H NMR and ^{13}C NMR spectra of OXCART synthesized in EDGE as a one-pot solvent.

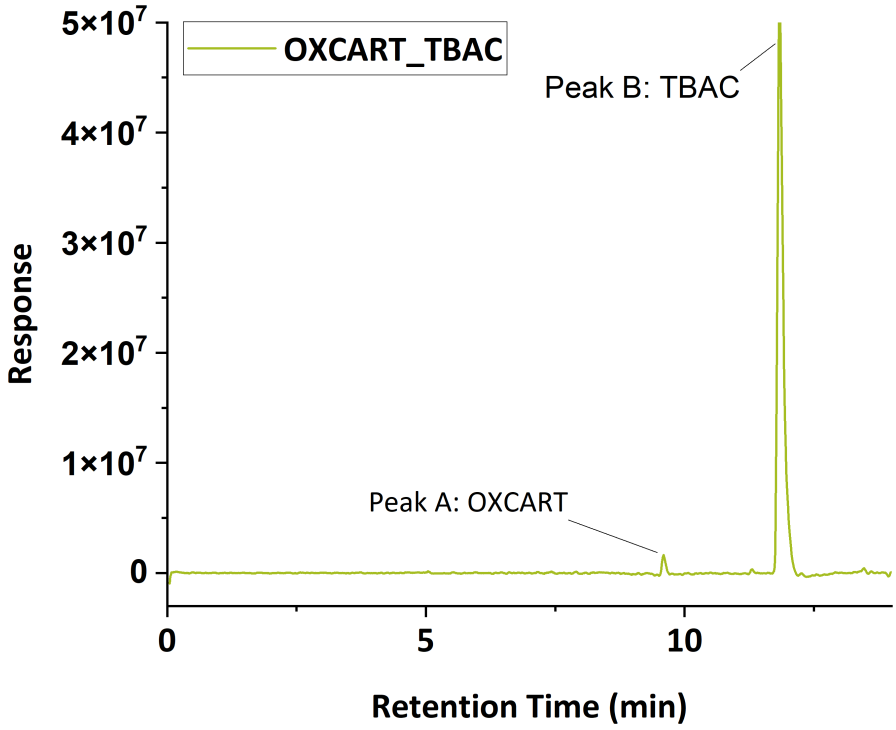

Figure S10: Chromatographic profile of OXCART synthesized in TBAC as a one-pot solvent

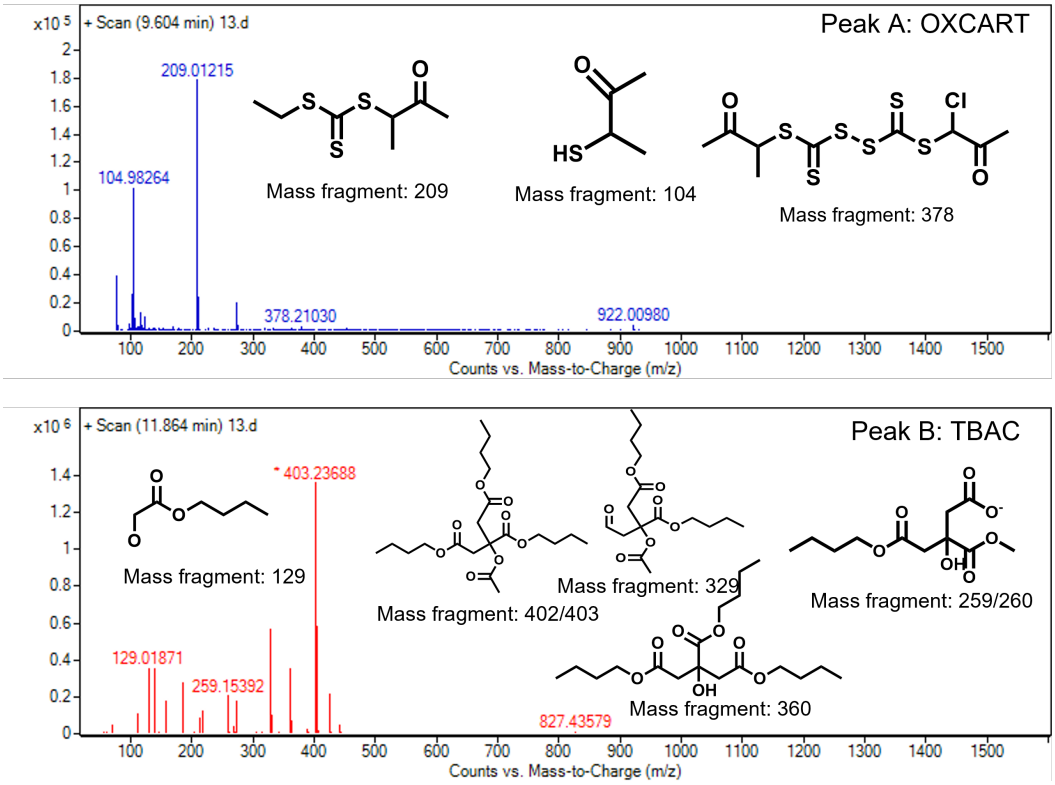

Figure S11: Mass spectra of OXCART synthesized in TBAC as a one-pot solvent

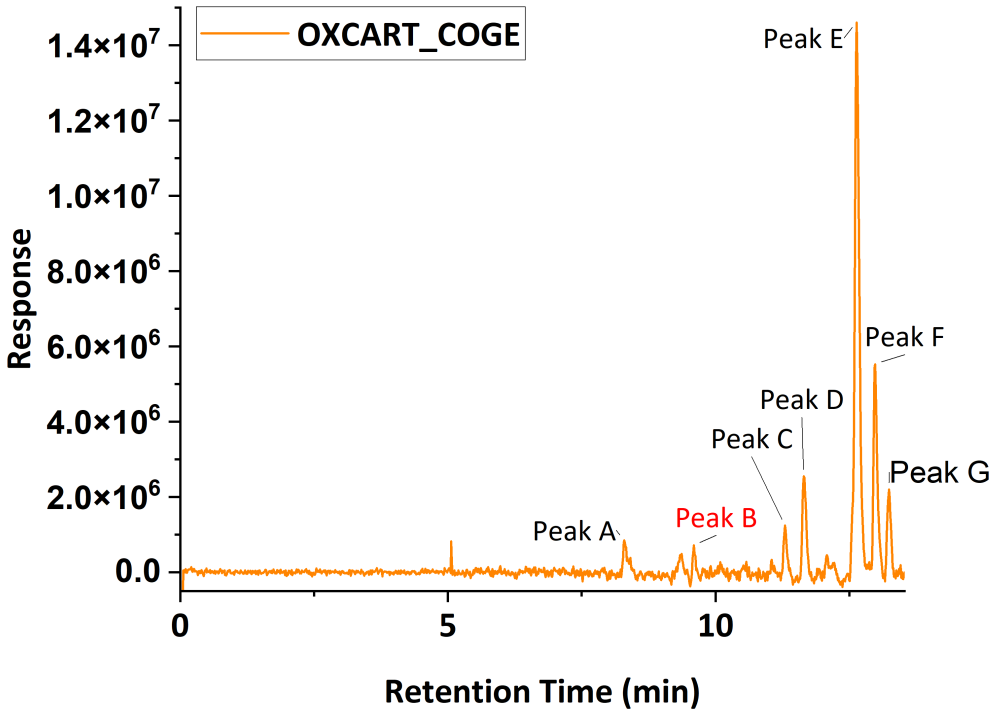

Figure S12: Chromatographic profile of OXCART synthesized in COGE as a one-pot solvent

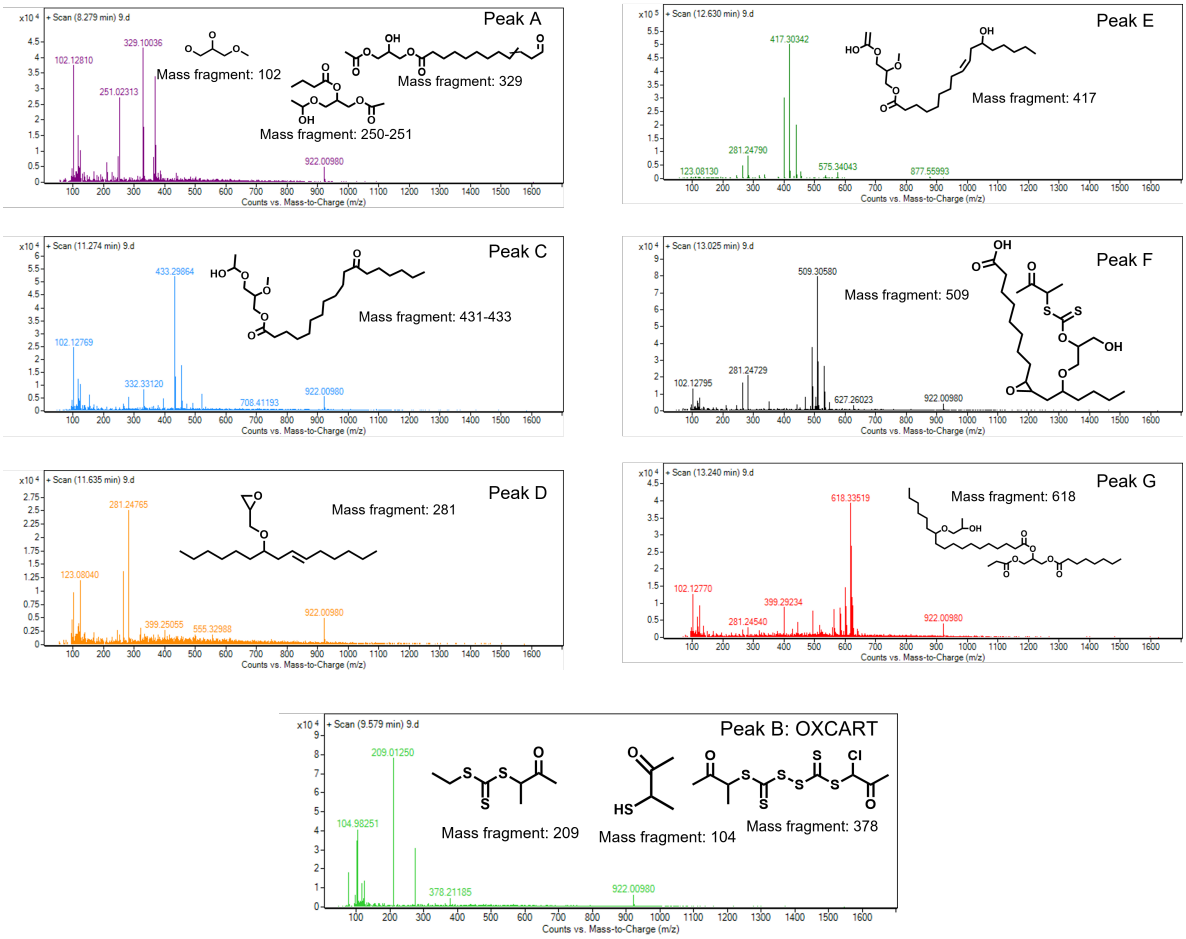

Figure S13: Mass spectra of OXCART synthesized in COGE as a one-pot solvent.

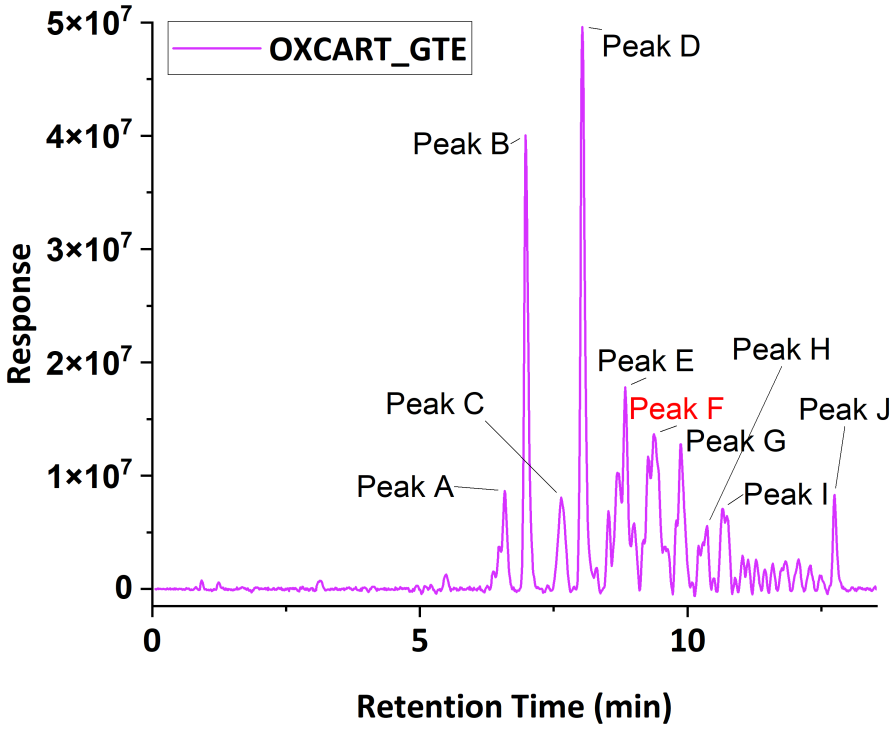

Figure S14: Chromatographic profile of OXCART synthesized in GTE as a one-pot solvent

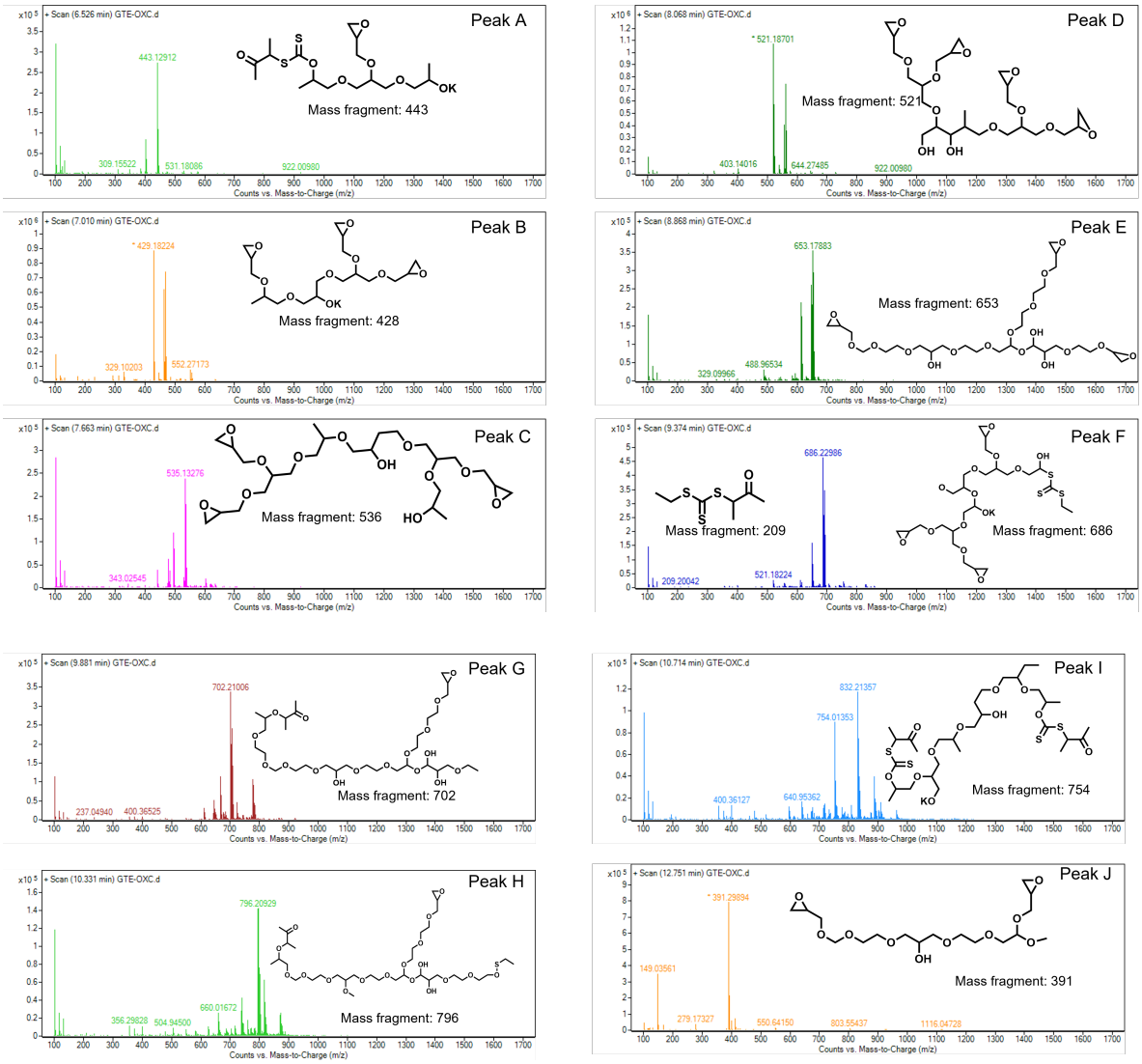

Figure S15: Mass spectra of OXCART synthesized in GTE as a one-pot solvent.

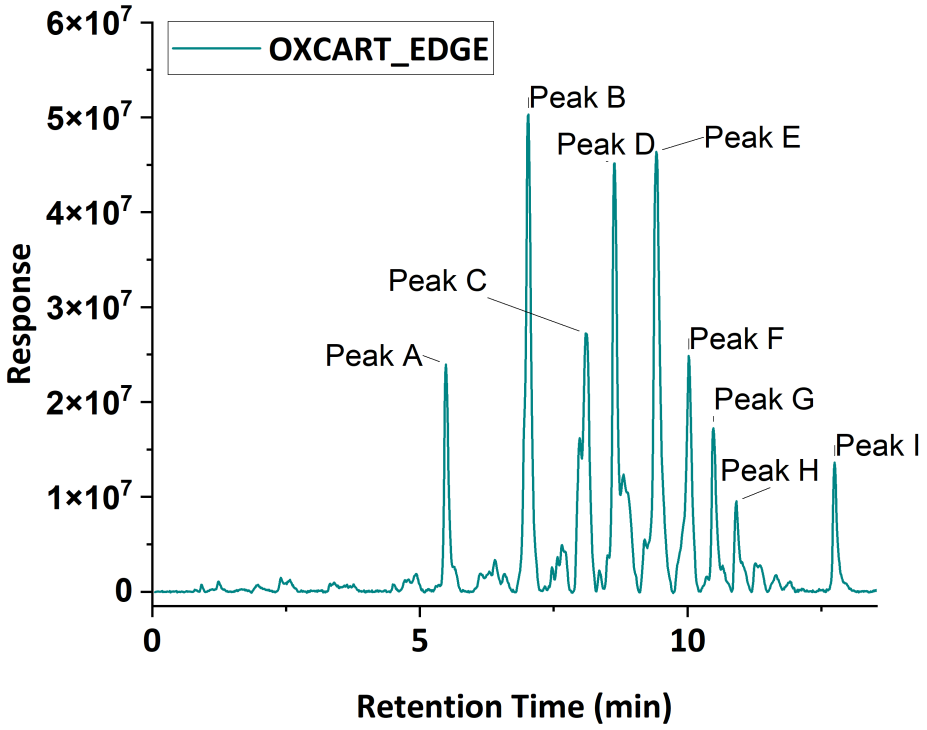

Figure S16: Chromatographic profile of OXCART synthesized in EDGE as a one-pot solvent

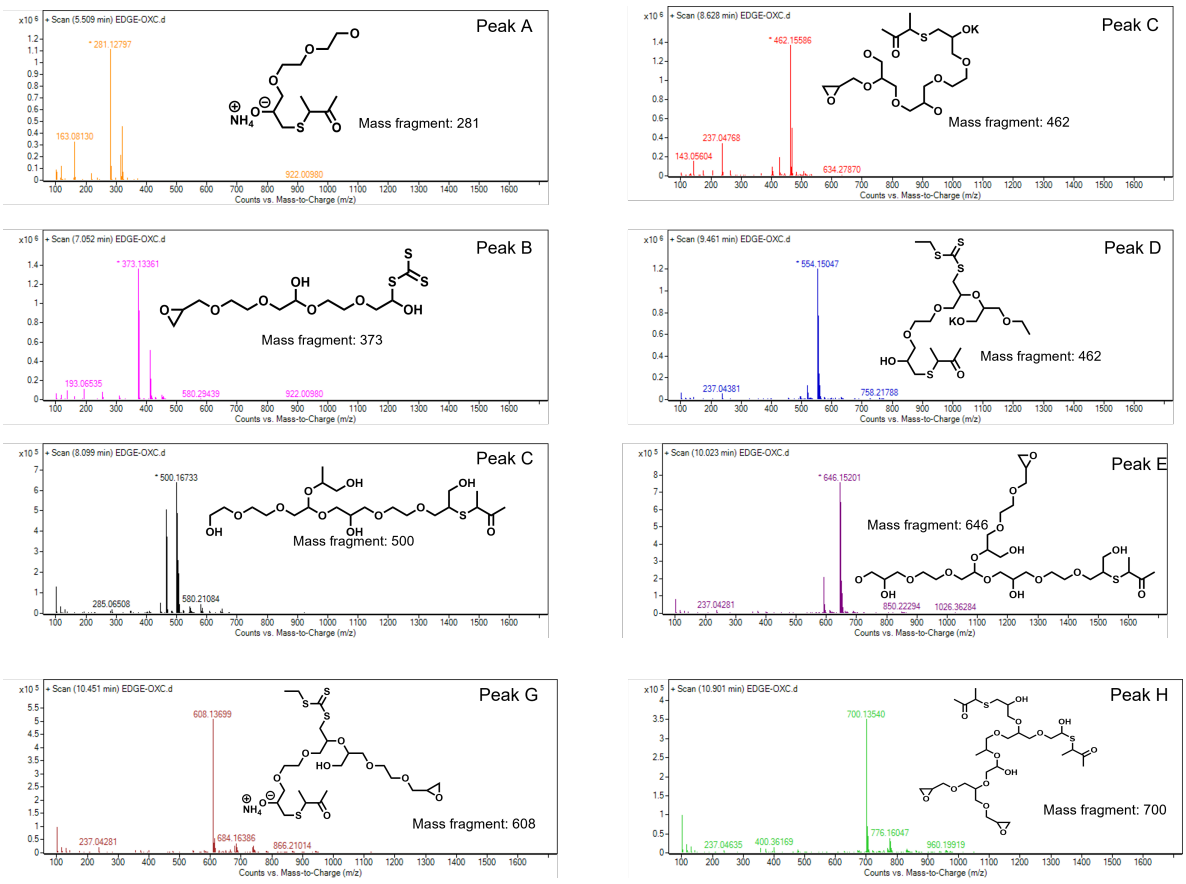

Figure S17: Mass spectra of OXCART synthesized in EDGE as a one-pot solvent.

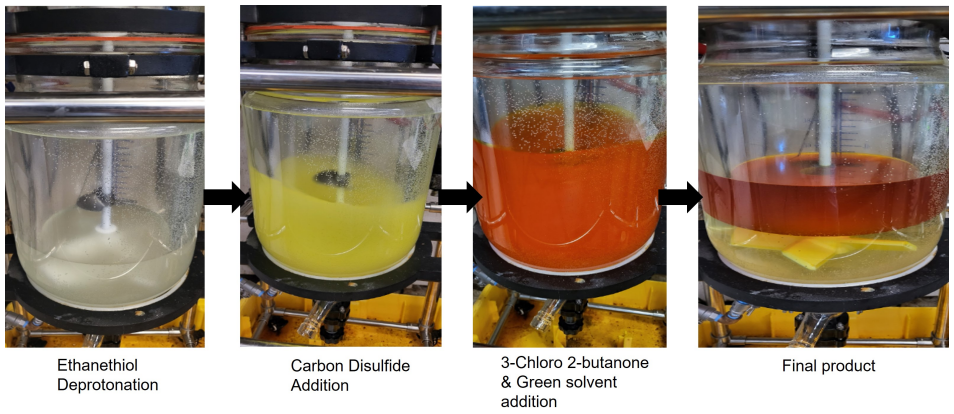

Figure S18: Schematic Representation of 10L synthesis of OXCART

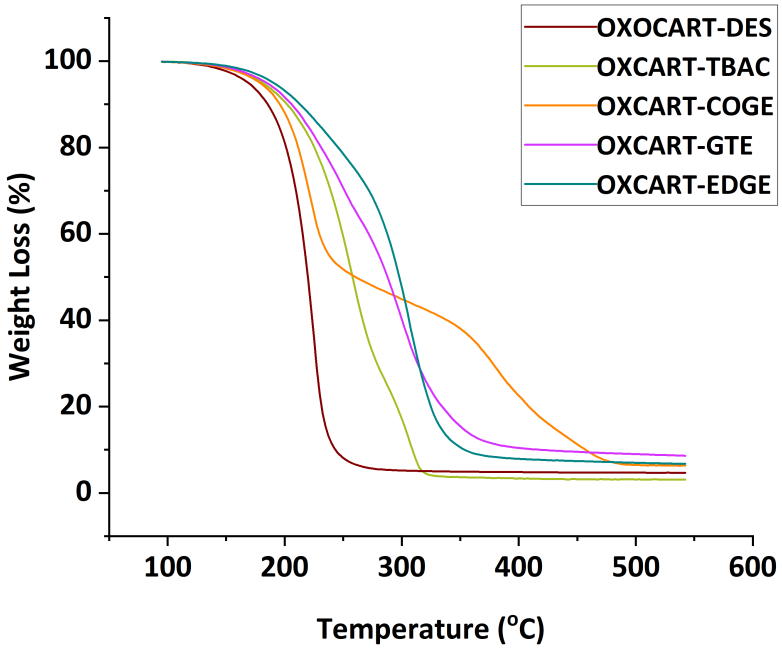

Figure S19: TGA thermograms showing percent mass loss in different variants of one-pot OXCART and OXOCART

Table S4: Thermogravimetric analysis of different one-pot OXCARTs and OXOCART

CTA	$t_{d5\%}$ (°C)	$t_{d50\%}$ (°C)	$t_{d90\%}$ (°C)
OXCART-TBAC	177.5	255	310
OXCART-COGE	177.5	260	457.5
OXCART-GTE	182.5	287.5	417.5
OXCART-EDGE	190	297.5	350
OXOCART-DES	167.5	219	242.5

Table S5: ^{1}H NMR integration and purity values for OXCART-DES for batch-to-batch variations

Batch	Peak a	Peak b	Peak c	Peak d	Peak e	Purity (%)	Dilution Factor
Batch 1	3.06	2.10	1.00	3.05	3.00	95	1.60
Batch 2	3.08	2.07	1.00	3.10	3.02	94	1.65
Batch 3	3.02	2.11	1.00	3.08	3.05	95	1.61
Batch 4	3.06	2.07	1.00	3.03	3.09	94	1.67
Batch 5	3.10	2.03	1.00	3.09	3.01	95	1.71

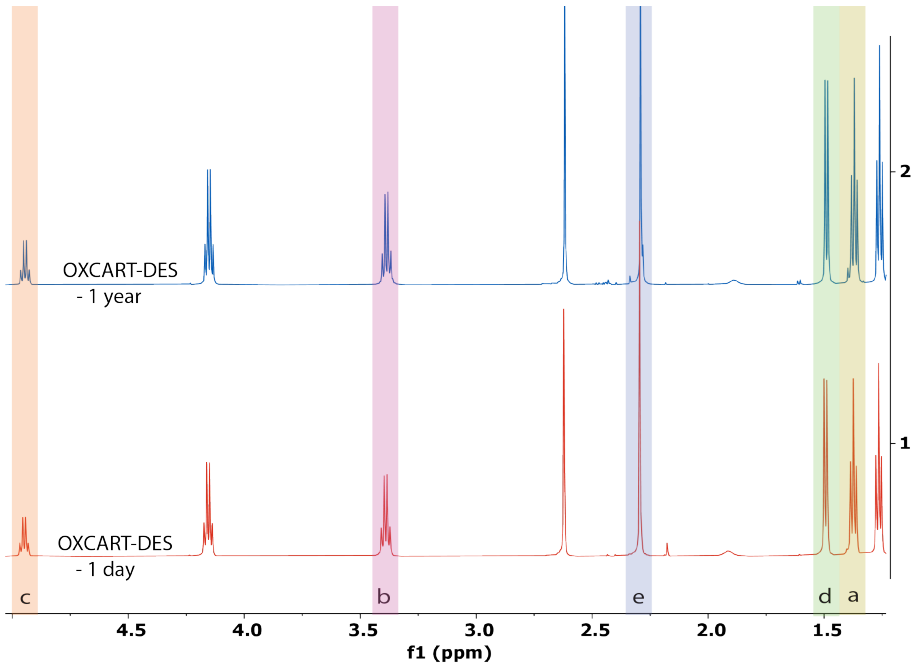

Figure S20: [1] H-NMR spectra comparison of OXCART synthesized in DES as a one-pot solvent for the same batch over a period of one year

Table S6: [1]H NMR integration and purity values for OXCART-DES for time-to-time variations

Time	**Peak a**	**Peak b**	**Peak c**	**Peak d**	**Peak e**	**Purity (%)**	**Dilution Factor**
1 year	3.08	2.09	1.00	3.05	3.05	94.8	1.60
1 day	3.08	2.07	1.00	3.05	3.02	95	1.60

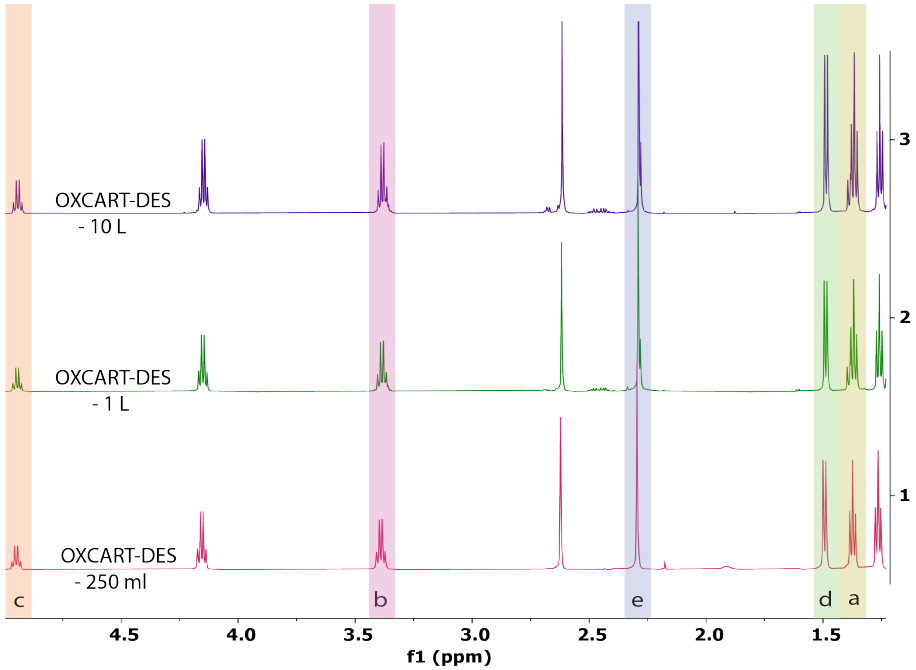

Figure S21: [1] H- NMR spectra comparison of OXCART synthesized in DES as a one-pot solvent at different scales

Table S7: [1]H NMR integration and purity values for OXCART-DES for scale-to-scale variations

Scale	**Peak a**	**Peak b**	**Peak c**	**Peak d**	**Peak e**	**Purity (%)**	**Dilution Factor**
10 L	3.07	2.06	1.00	3.11	3.02	94	1.63
1 L	3.11	2.10	1.00	3.04	3.05	94	1.65
250 ml	3.08	2.07	1.00	3.05	3.02	95	1.60

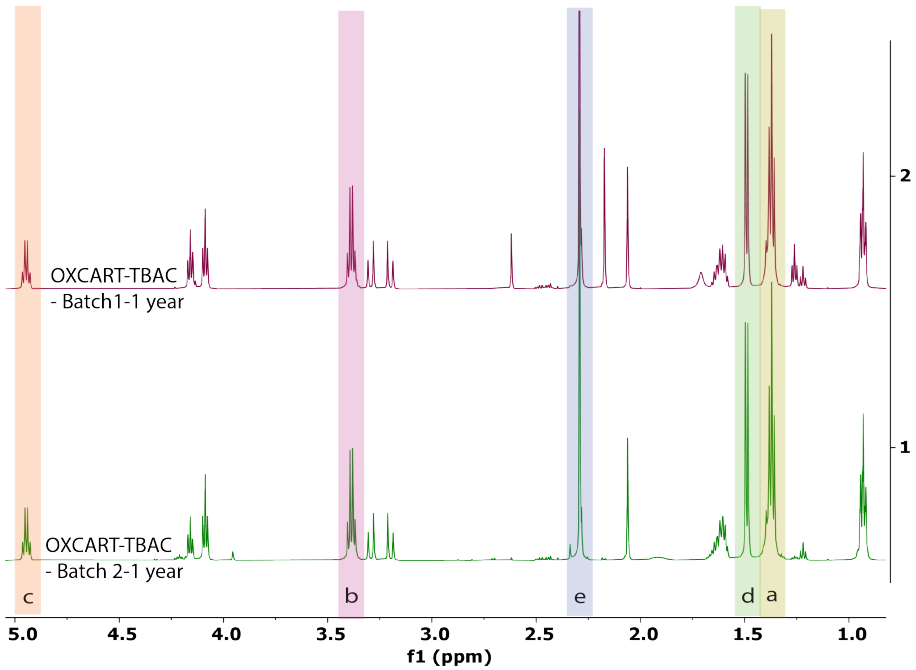

Figure S22: ^{1} H- NMR spectra comparison of OXCART synthesized in TBAC as one-pot solvent for 2 different batches kept for 1 year

Table S8: ^{1}H NMR integration and purity values for OXCART-TBAC for batch-to-batch and time-to-time variations

Time	**Peak a**	**Peak b**	**Peak c**	**Peak d**	**Peak e**	**Purity (%)**	**Dilution Factor**
Batch 1-1 year	3.41	2.12	1.00	3.04	3.09	90	2.15
Batch 2-1 year	3.51	2.02	1.00	3.05	3.03	93	2.05

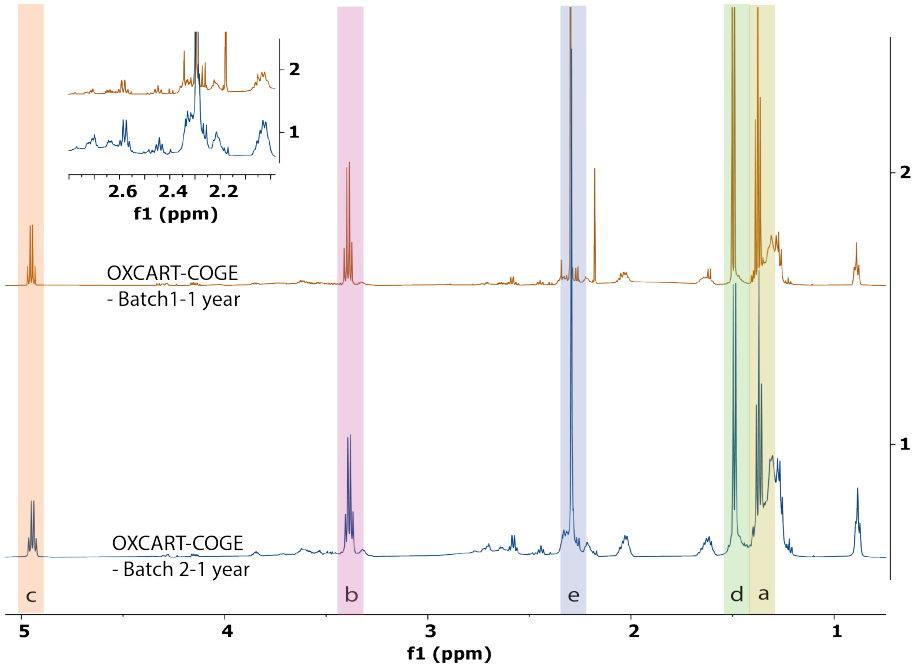

Figure S23: [1] H- NMR spectra comparison of OXCART synthesized in COGE as a one-pot solvent for 2 different batches kept for 1 year

Table S9: [1]H NMR integration and purity values for OXCART-COGE for batch-to-batch and time-to-time variations

Time	**Peak a**	**Peak b**	**Peak c**	**Peak d**	**Peak e**	**Purity (%)**	**Dilution Factor**
Batch 1-1 year	3.50	2.24	1.00	3.32	3.03	60	3.05
Batch 2-1 year	3.81	2.38	1.00	3.45	3.09	52	3.5

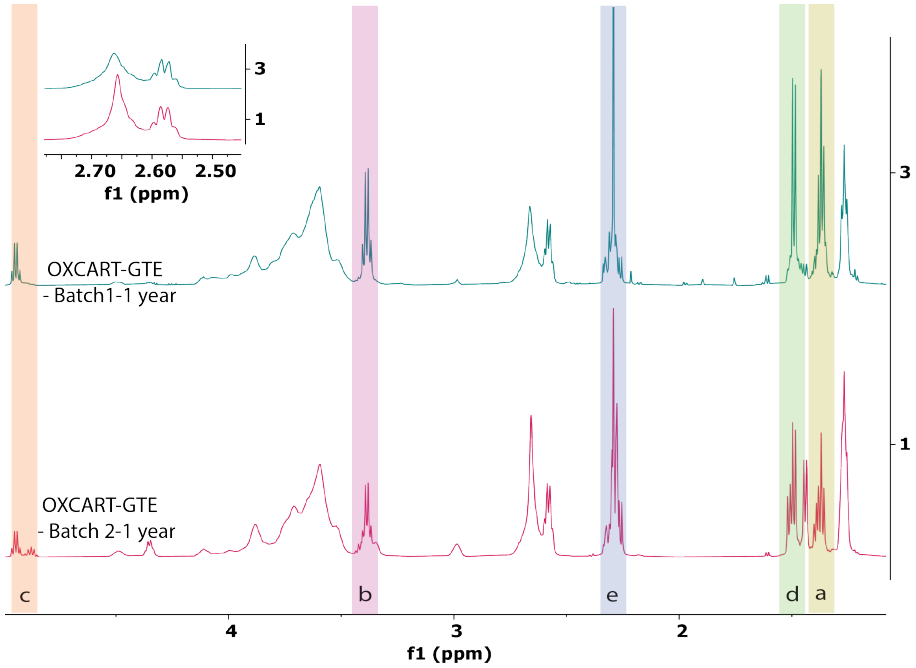

Figure S24: [1] H- NMR spectra comparison of OXCART synthesized in GTE as a one-pot solvent for 2 different batches kept for 1 year

Table S10: [1]H NMR integration and purity values for OXCART-GTE for batch-to-batch and time-to-time variations

Time	**Peak a**	**Peak b**	**Peak c**	**Peak d**	**Peak e**	**Purity (%)**	**Dilution Factor**
Batch 1-1 year	3.38	2.61	1.00	3.05	3.03	32	4.05
Batch 2-1 year	3.62	2.68	1.00	3.15	3.29	12	5.1

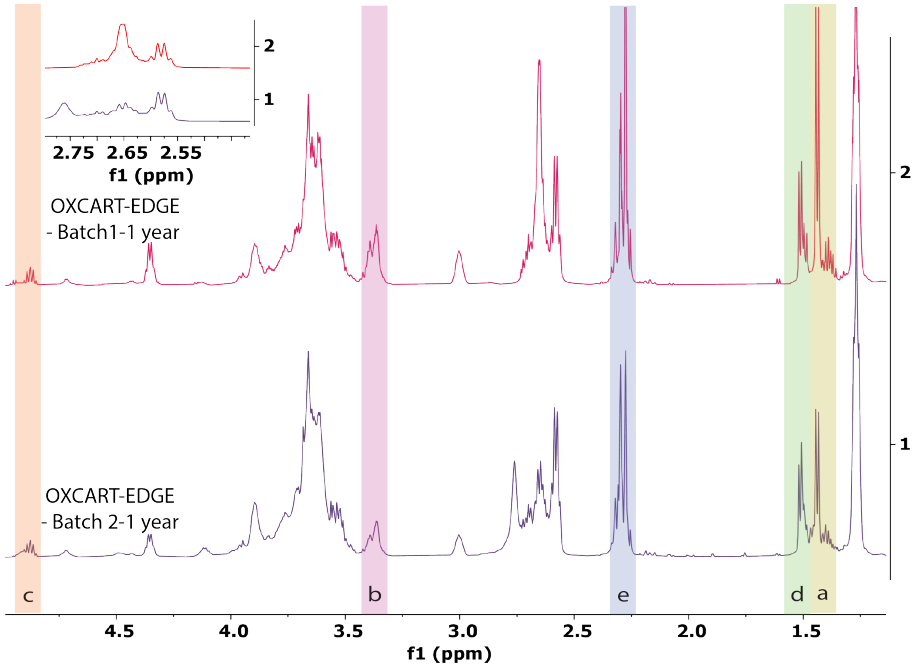

Figure S25: [1] H- NMR spectra comparison of OXCART synthesized in EDGE as a one-pot solvent for 2 different batches kept for 1 year

Table S11: [1]H NMR integration and purity values for OXCART-EDGE for batch-to-batch and time-to-time variations

Time	**Peak a**	**Peak b**	**Peak c**	**Peak d**	**Peak e**	**Purity (%)**	**Dilution Factor**
Batch 1-1 year	3.22	2.31	1.00	3.25	3.53	5.6	10.05
Batch 2-1 year	3.42	2.48	1.00	3.45	3.69	5.1	11.1

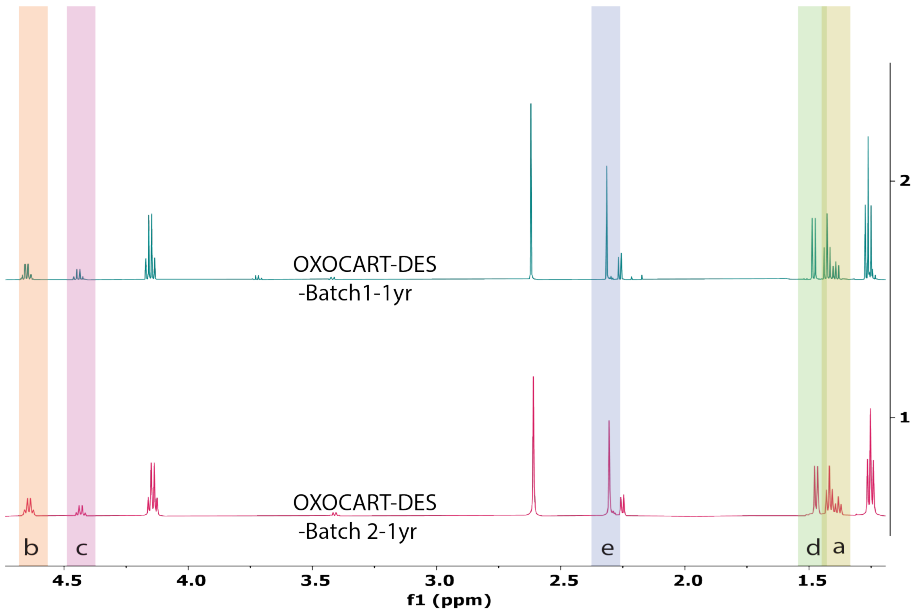

Figure S26: [1] H- NMR spectra comparison of OXOCART synthesized in DES as one-pot solvent for 2 different batches kept for 1 year

Table S12: [1]H NMR integration and purity values for OXOCART-DES for batch-to-batch and time-to-time variations

Time	**Peak a**	**Peak b**	**Peak c**	**Peak d**	**Peak e**	**Purity (%)**	**Dilution Factor**
Batch 1-1 year	3.06	2.00	0.99	3.00	3.07	94	1.71
Batch 2-1 year	3.08	2.01	1.00	3.05	3.09	93.2	1.81

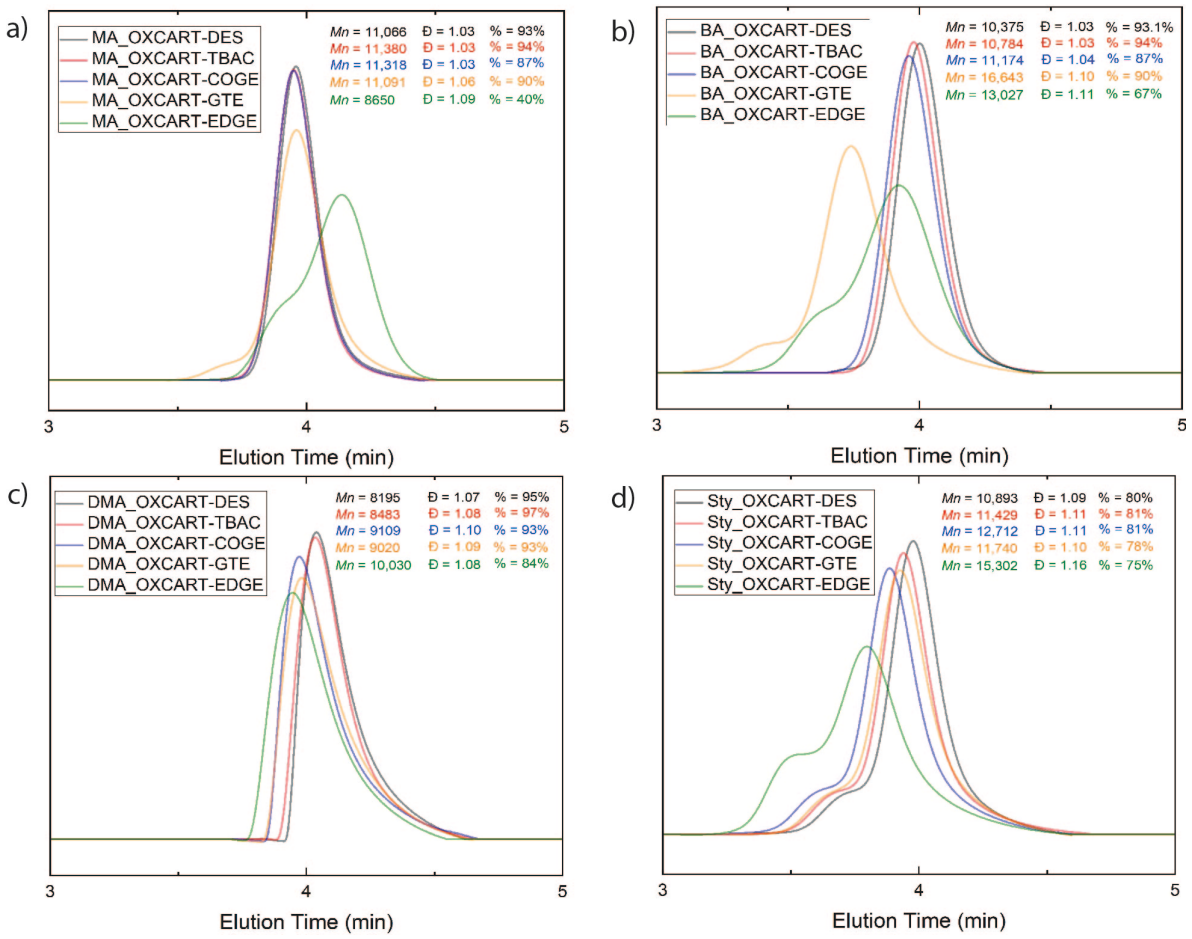

Figure S27: SEC chromatograms of methyl acrylate, butyl acrylate, dimethyl acrylamide, and styrene polymerized using different types of one-pot OXCART

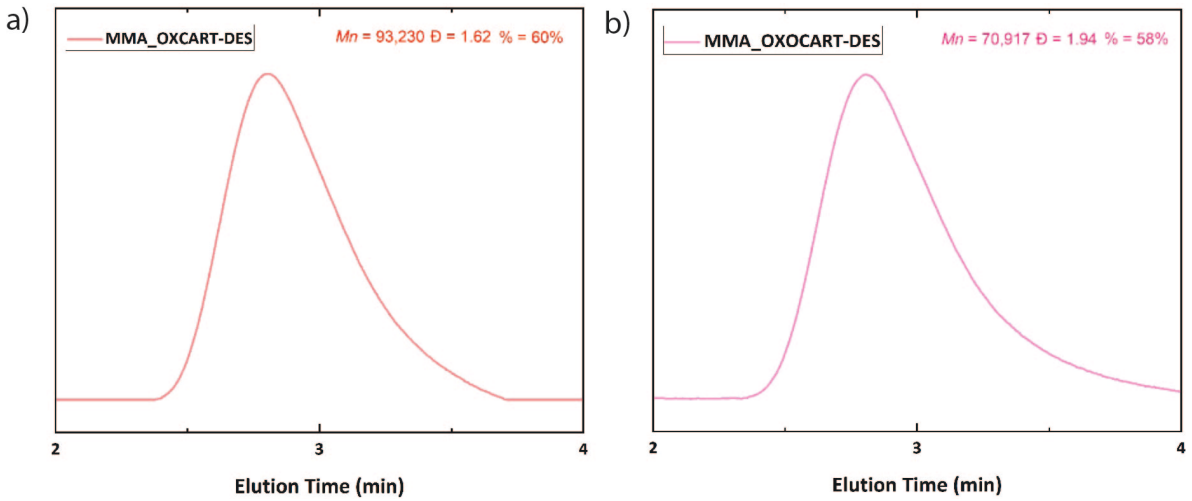

Figure S28: SEC chromatograms of methyl methacrylate polymerized using OXCART-DES and OXOCART-DES

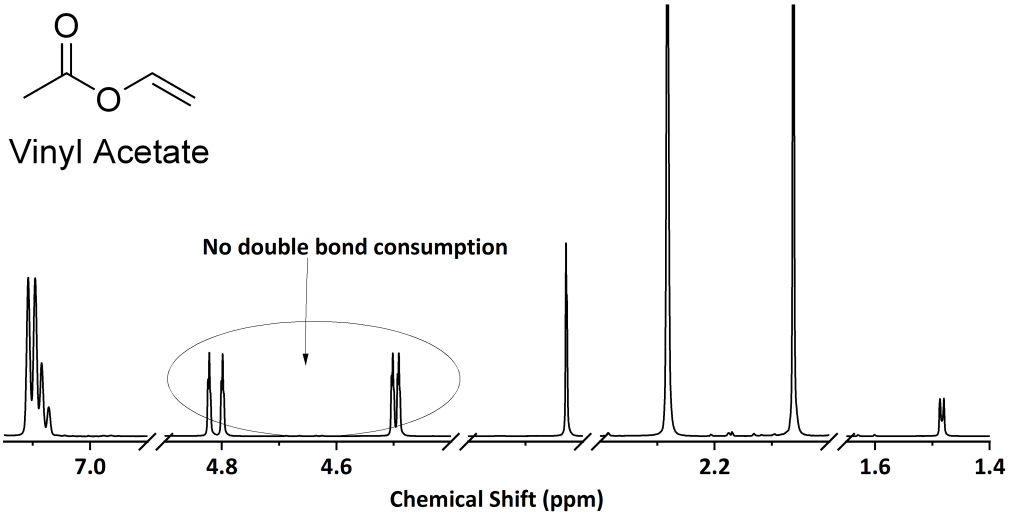

Figure S29: ^{1}H NMR spectra of Vinyl Acetate after 8hrs of polymerization using OXCART-DES

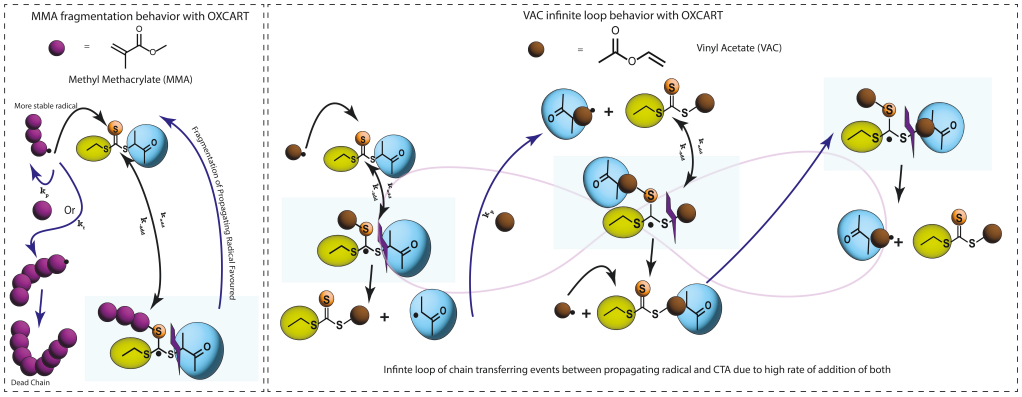

Figure S30: Reaction mechanism showing the uncontrolled chain transferring and termination of MMA and infinite looping of VAC radicals using trithiocarbonate-based CTA

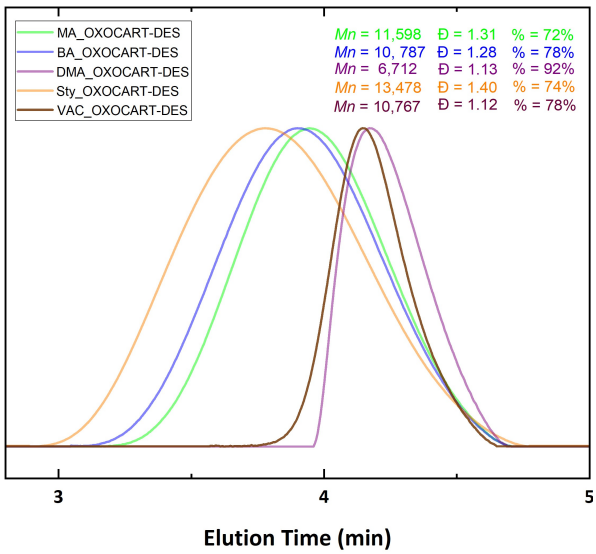

Figure S31: SEC chromatograms of methyl acrylate, butyl acrylate, dimethyl acrylamide, styrene, and vinyl acetate polymerized using OXOCART-DES

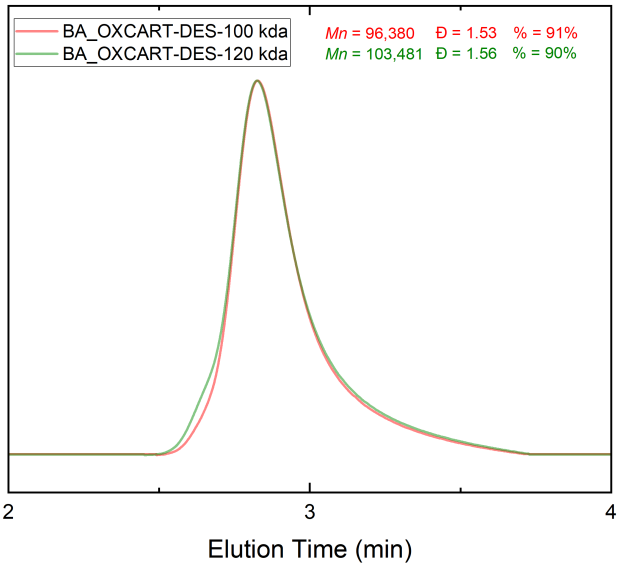

Figure S32: SEC chromatograms of butyl acrylate polymerized using OXCART-DES with higher targeted molecular weights

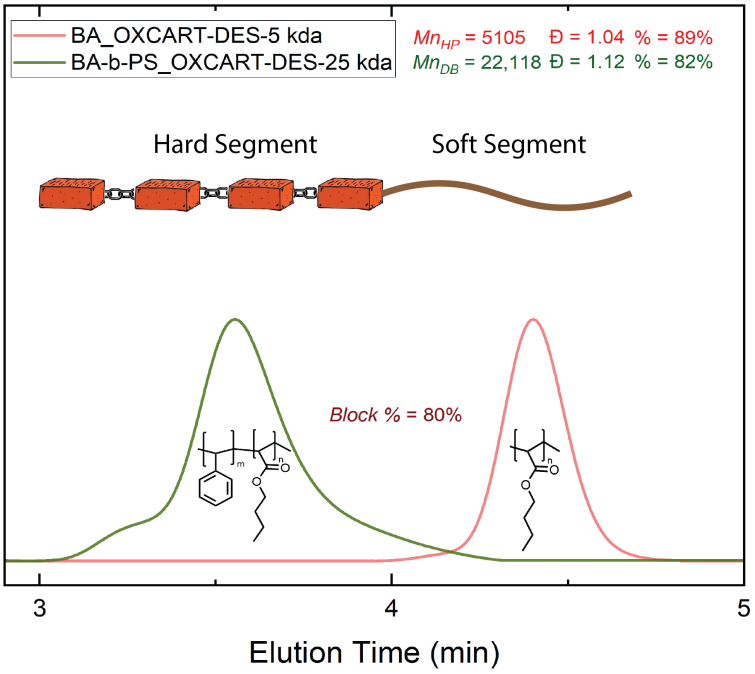

Figure S33: SEC chromatograms of a butyl acrylate-based macro-CTA and the subsequent hard styrene block grown over the macro-CTA